Thermal Metamorphism in Chondrites

Gary R. Huss
Arizona State University

Alan E. Rubin
University of California, Los Angeles

Jeffrey N. Grossman
U.S. Geological Survey

Thermal metamorphism has affected most chondritic meteorites to some extent, and in most ordinary chondrites, some carbonaceous chondrites, and many enstatite chondrites it has significantly modified the primary characteristics of the meteorites. Metamorphic grade, as described by the petrologic type, is one axis of the current two-dimensional system for classifying chondrites. Many changes are produced during thermal metamorphism, including textural integration and recrystallization, mineral equilibration, destruction of primary minerals, and growth of secondary minerals. Understanding these changes is critical if one hopes to infer the conditions under which chondrites originally formed. In addition to summarizing metamorphic changes, we also discuss temperatures, oxidation states, and possible heat sources for metamorphism.

1. INTRODUCTION

Once the various chondrite components had formed, they accreted into meteorite parent bodies. Starting with accretion itself, secondary processes such as shock metamorphism, thermal metamorphism, and aqueous alteration began to modify the primary chondritic components. The nature and pervasiveness of secondary processing must be understood before currently observed properties of chondrites and their components can be used to infer the nature of the solar nebula. In this chapter, we discuss the effects of thermal metamorphism on chondritic meteorites and the conditions under which it occurred. Thermal metamorphism affected most chondrite classes, and its effects play a major role in the classification schemes that have been developed for chondrites (see *Weisberg et al.,* 2006).

Thermal metamorphism is a broad topic without sharp boundaries. For example, heating due to the passage of a shock wave potentially affects components of a meteorite in the same way as heat provided by gravitational compression or radioactive decay. In addition, the style of thermal metamorphism is affected by the presence of water, so it is difficult to set a firm boundary between aqueous alteration and thermal metamorphism. In this chapter, we will mainly discuss the changes induced by heating on the meteorite parent bodies over a long timescale. The pervasive aqueous alteration that affected CI and CM chondrites, and to a lesser extent CR and other carbonaceous chondrites, is covered in the next chapter. However, we will discuss the effects of small amounts of water during the metamorphism of type 3 ordinary chondrites and CO3 chondrites. Although shock metamorphism is not covered in detail, we will mention some of its effects in order to distinguish them as far as possible from the effects of thermal metamorphism.

The current classification system for chondrites is based on the scheme proposed by *Van Schmus and Wood* (1967). These authors divided chondrites into compositional groups and divided the compositional groups into six petrologic types. Petrologic types 3–6 were viewed as reflecting the level of thermal metamorphism, whereas types 1 and 2 were used to designate unmetamorphosed meteorites unrelated to types 3–6. Types 1 and 2 have experienced different degrees of aqueous alteration (e.g., *McSween,* 1979). All well-defined chondrite groups contain little-metamorphosed members. However, many groups of carbonaceous chondrites have no known members of petrologic type ≥ 4 (e.g., CI, CM, CO, CV, CR, CH).

The petrologic types in the original *Van Schmus and Wood* (1967) classification have been modified in several ways in the nearly 40 years since they were proposed. A few dozen meteorites have been classified as type 7 [e.g., Shaw (*Dodd et al.,* 1975), Happy Canyon (*Olsen et al.,* 1976)]. Many of these meteorites probably are (or contain) impact melts (e.g., *Taylor et al.,* 1979; *McCoy et al.,* 1995) and thus are not part of the continuum of thermal metamorphism. For these meteorites, a type 7 designation is inappropriate, since shock stage is classified independently (*Stöffler et al.,* 1991; *Scott et al.,* 1992). Other chondritic meteor-

ites have been heated to the point of partial melting and are possibly metamorphic rocks of higher grade than type 6. These are known as "primitive achondrites," and are beyond the scope of this chapter. But there are a few highly metamorphosed chondrites, such as Lewis Cliff 88663, that satisfy the *Dodd et al.* (1975) criteria for type 7 without evidence for shock melting or partial melting (*Mittlefehldt and Lindstrom,* 2001). These can conceivably be called type 7 chondrites, although they do fit comfortably within the *Van Schmus and Wood* (1967) definition of type 6. We choose not to make any distinction between these in the following discussion.

A second extension of the *Van Schmus and Wood* (1967) classification involves dividing type 3 into subtypes, 3.0 to 3.9, where type 3.0 designates meteorites that have experienced very little metamorphism and 3.9 designates those that have nearly reached the degree of chemical equilibrium associated with type 4. This scheme was originally proposed by for ordinary chondrites by *Sears et al.* (1980), and has since been extended to several other chondrite groups, including CO (*Scott and Jones,* 1990; *Sears et al.,* 1991a; *Chizmadia et al.,* 2002), CV (e.g., *Guimon et al.,* 1995; *Bonal et al.,* 2004), and R (e.g., *Rubin and Kallemeyn,* 1989; *Bischoff,* 2000).

In this chapter, we discuss the chemical and mineralogical changes in chondrites of all groups, first during the early stages of metamorphism from types 3.0 to 3.9, and then at higher grades represented by types 4–6, as metamorphism proceeds to near the point of partial melting. We conclude with a discussion of the conditions and timescales of metamorphism and the processes responsible for the heating.

2.   LOW-DEGREE METAMORPHISM (TYPE 3 CHONDRITES)

2.1.   Type 3 Ordinary Chondrites

Type 3 ordinary chondrites, although often considered unmetamorphosed, show a wide range of metamorphic effects. *Wood* (1967) identified a population of primitive chondrites, including several ordinary chondrites, that do not show a coherent relationship between taenite composition and grain size (indicative of slow cooling). He concluded that these were "more lightly touched by metamorphism than the other[s]." *Dodd et al.* (1967) and *Dodd* (1969) described the characteristics of several ordinary chondrites designated as type 3 by *Van Schmus and Wood* (1967) that seemed less equilibrated than others. *Huss et al.* (1978, 1981) attempted to arrange type 3 ordinary chondrites in a metamorphic sequence based on the degree of recrystallization and homogenization of olivine compositions in the fine-grained matrix. Shortly thereafter, *Afiattalab and Wasson* (1980) observed that the Co contents of metal grains also vary systematically with degree of metamorphic heating. *Sears et al.* (1980) discovered that bulk thermoluminescence (TL) sensitivity is an excellent indicator of metamorphic grade in type 3 ordinary chondrites;

they used this parameter to define the modern petrologic types, 3.0–3.9 (see also *Sears et al.,* 1982a; *Sears et al.,* 1991b; *Benoit et al.,* 2002). *Grossman and Brearley* (2005) studied the effects of very low degrees of metamorphism on olivine and glass composition, opaque mineralogy, and matrix composition in order to define petrologic types 3.00–3.15. A summary of the modern petrologic classification scheme for ordinary chondrites and the characteristic properties of each type is given in Table 1.

2.1.1.   Physical effects (thermoluminescence and cathodoluminescence).   Thermoluminescence sensitivity is the amount of TL that is induced in a sample by irradiation under standard conditions. Thermoluminescence sensitivity varies by ~3 orders of magnitude among type 3 ordinary chondrites and is correlated with all metamorphic indicators noted by earlier workers (Table 1), including degree of matrix recrystallization, olivine heterogeneity, matrix and metal compositions, and bulk volatile contents (C and ^{36}Ar) (*Sears et al.,* 1980, 1982a). Differences in TL sensitivity among type 3 ordinary chondrites are due mainly to crystallization of feldspar during metamorphism, primarily via devitrification of chondrule glass (*Sears et al.,* 1980, 1982a), but also via recrystallization of matrix (*Huss et al.,* 1981).

The shape of the TL-sensitivity glow curve (TL sensitivity plotted vs. the temperature of emission) varies as a function of metamorphic grade in type 3 ordinary chondrites (*Sears et al.,* 1980, 1982a). Below type 3.3, the shape of the glow curve is irregular. Between 3.3 and 3.5, a well-defined peak develops. Between types 3.5 and 3.6, this peak broadens and moves to higher temperature, probably due to the order/disorder transition of feldspar that occurs at 500°–600°C (*Guimon et al.,* 1985; *Sears et al.,* 1991b). The irregular shape of the glow curve below type 3.3 may reflect dominance of phosphors other than feldspar in meteorites whose metamorphic temperatures were too low for extensive feldspar growth (e.g., *Guimon et al.,* 1988).

Cathodoluminescence (CL) is visible light emitted by minerals in response to an electron beam. The CL properties of type 3 ordinary chondrites also vary greatly in response to metamorphism [see photomicrographs in *Sears et al.* (1990)]. Low-FeO chondrules containing glass with bright yellow CL are found only in the lowest petrologic types, such as Semarkona (LL3.00), Bishunpur (LL3.15), and Krymka (LL3.2) [petrologic types from *Grossman and Brearley* (2005)]. By type 3.4, the mesostasis in low-FeO chondrules shows only blue CL (*DeHart et al.,* 1992; *Sears et al.,* 1995). With increasing petrologic type, the proportion of chondrules showing blue CL increases, and the matrix also begins to luminesce blue. This behavior parallels that shown by TL and is due to the growth of blue-luminescing albitic plagioclase (*Grossman and Brearley,* 2005). Olivine showing red CL (forsterite) is common in petrologic types ≤3.4, but disappears at higher grades, reflecting the entry of FeO during metamorphism (*Sears et al.,* 1990). Fine-grained matrix forsterite is lost by type ~3.2, while coarser chondrule forsterite is gone by type ~3.6. The matrix of the least-metamorphosed ordinary chondrite,

TABLE 1. Summary of petrologic types of ordinary chondrites.

Category	Parameter	Petrologic types													Discussed in Section
		3.0	3.1	3.2	3.3	3.4	3.5	3.6	3.7	3.8	3.9	4	5	6	
Bulk composition	Carbon (wt%)	0.3–0.6						0.2–0.5				<0.3			§2.1.5
	H₂O (wt%)	1.0–2.5										<1.0			MetBase*
	Indium (ppb)	8–100											0.1–8		
	$^{36}Ar_p$ (10⁻⁸ g⁻¹ STP)	45–60			15–50					5–15		0.5–5		0.2–2	
Texture	Chondrule textural equilibration	None		Incipient					Noticeable			Minor	Moderate	Extensive	§3.1.1
Thermoluminescence	Sensitivity (×1000, rel. Dhajala)	<1	1–2.2	2.2–4.6	4.6–10	10–22	22–46	46–100	100–220	220–460		300–600	600–2000		§2.1.1
	Glowcurve shape	Irregular								Sharp peak					
	Peak temperature	170–200			<140					>140					
Cathodoluminescence	Yellow CL in chondrule mesostasis	Common			Rare					Absent					§2.1.1
	Blue CL in chondrule mesostasis	Present			Common					Dominant					
	Red CL in chondrule olivine	Red	Red areas		Low CL			Rare to absent		Increasingly blue			Absent		
	Matrix CL												Matrix absent		
Matrix	Hydrated phases	Abundant	Present						Absent				Matrix absent		§2.1.2
	Presolar graphite		Present						Absent				Matrix absent		
	Presolar diamonds		Present		Decreasing					Absent			Matrix absent		
	F/FM†	>1.4						1.1–1.4		<1.1			Matrix absent		
	Matrix recrystallization (%)		<20	>20								100	Matrix absent		
	Sulfur content (wt%)	>1.0	0.5–1.0						<0.5				Matrix absent		
Feldspathic material	Texture of chondrule mesostasis					Number density of crystallites increases					Recrystallized				§2.1.3 / §3.1.2
	Isotropic glass	Common						Less common		Rare		Absent			
	Type I chondrule mesostasis	Modal albite uncommon				Normative anorthite decreases			Modal albite present			Mesostasis absent			
	Type II chondrule mesostasis	Albite rare				Modal albite increases			Modal albite present			Mesostasis absent			
	Grain size secondary feld (μm)	Submicrometer								2		2	2–10	50	
Olivine	PMD‡ Fa (%)	>33		15–3	20–3			3		5–15			<5		§2.1.3
	Type I chondrules	FeO < 2 wt%				FeO converges to equilibrium value			FeO increases to equilibrium value		Near equilibrium	Near equilibrium	Uniform		
	Type II chondrules	CaO > 0.3 wt% common							CaO decreases to equilibrium value		Near equilibrium	Near equilibrium	Uniform		
Pyroxene	PMD* Fs in low-Ca pyroxene (%)	Cr₂O₃ > 0.3 wt%	>30		20–3				Cr₂O₃ > 0.1 wt%		0	5–20	<5		§2.1.3 / §3.1.2 / §3.1.3
	Structure of low-Ca pyroxene			Predominantly monoclinic								Mixed	Orthorhombic		
	Grain-size of high-Ca pyroxene (μm)	Cr₂O₃ > 0.3 wt% heter.			Small grain in chondrule mesostasis							<1	2–5	5–30	
Nonsilicates	Phosphates	Some Na- and Fe-rich							Ca-rich, increasing abundance and grain size				Large grains Ca-phosphate		§2.1.4 / §3.1.2 / §3.1.4
	Kamacite	Co heterogeneity high							Co heterogeneity moderate				Co heterogeneity low		
	Taenite	P, Cr, Si-bearing		Unzoned					Zoned			P, Cr, Si-free			
	Carbides, magnetite	Common			Present					Rare to absent					

*Compiled from data in MetBase 7.1, a comprehensive meteorite database marketed by *Köblitz* (2005). Primordial ³⁶Ar calculated from ³⁶Ar and ³⁸Ar abundances assuming primordial ³⁶Ar/³⁸Ar = 5.6 and spallogenic ³⁶Ar/³⁸Ar = 0.65. Sharps was excluded from ranges due to its anomalously high volatile-element content, probably carried by abundant C- and S-rich xenoliths (J. Grossman, unpublished data).
†FeO/(FeO + MgO) in matrix, normalized to whole rock.
‡PMD = percent mean deviation, defined by *Dodd et al.* (1967) as the mean deviation of the iron concentration (wt%) in individual measurements of olivine or pyroxene from the mean of these measurements divided by the average iron content (wt%) multiplied by 100. Literature data probably dominated by grains in chondrules and chondrule fragments, but may include some in matrix.

Solid vertical lines represent criteria that are most important in distinguishing adjacent subtypes. All increases and decreases are noted run from low to high petrologic types. The listed ranges of petrologic types associated with each parameter in this table were determined by the present authors based on primary literature data except for TL sensitivity in types 3.2–3.9, which are quoted from *Sears et al.* (1980) and the cutoff in PMD of olivine between types 3.9 and 4, which is taken directly from *Van Schmus and Wood* (1967). See the indicated text section for references.

Semarkona, shows a pervasive smoky-red CL (*DeHart et al.,* 1992). This property is less pronounced in type 3.1 chondrites, and is absent in higher types.

2.1.2. Effects in fine-grained matrix. Evidence of post-accretionary alteration in the matrix of type 3 ordinary chondrites was found in the first detailed studies to utilize the power of the scanning electron microscope (*Christophe Michel-Levy,* 1976; *Ashworth and Barber,* 1976; *Ashworth,* 1977). Later studies identified a series of changes in optical properties, mineralogy, and degree of chemical equilibration that could be confidently attributed to thermal metamorphism (*Huss et al.,* 1981; *Nagahara,* 1984; *Grossman and Brearley,* 2005). Recent work has also given us some idea of what the original, unmetamorphosed matrix material might have looked like.

In type 3.0–3.2 ordinary chondrites, matrix is opaque in standard thin sections. The very mild thermal metamorphism experienced by these meteorites has proceeded in the presence of varying amounts of water. In Semarkona (LL3.00) matrix, most of the primary silicates and sulfides have been converted to phyllosilicates and Ni-rich pyrrhotite (*Hutchison et al.,* 1987; *Alexander et al.,* 1989a). This assemblage gives Semarkona matrix a translucent brown to olive-green color in very thin (~10 μm) sections (*Hutchison et al.,* 1987). In Bishunpur (LL3.15), the matrix contains Na-, Al-, and Si-rich amorphous material instead of phyllosilicate (*Alexander et al.,* 1989a). Such material is highly susceptible to aqueous alteration and in Semarkona was probably converted to phyllosilicates. It survives in Bishunpur because less water was present. Type 3.0–3.2 chondrites contain micrometer-sized matrix olivine grains. In Semarkona, the compositions of these olivine grains range from 2 mol% fayalite [molar FeO/(FeO + MgO)] (Fa_2) to Fa_{40}, whereas in Bishunpur and Krymka (LL3.2), matrix olivines range from Fa_{25} to Fa_{90} (*Huss et al.,* 1981; *Nagahara,* 1984). These olivines were probably produced *in situ* from amorphous material and phyllosilicate (*Alexander et al.,* 1989a,b; *Scott and Krot,* 2003), and the more-restricted range of Semarkona matrix olivines may be a consequence of more-extensive aqueous alteration. Semarkona matrix also exhibits pervasive red CL (*Sears et al.,* 1990) that probably reflects a significant abundance of tiny forsterite grains. These grains are much less abundant in Bishunpur and are apparently absent in Krymka; they may have been converted to Fe-rich olivine by mild thermal metamorphism.

In petrologic types above 3.2, thermal metamorphism seems to have proceeded without the aid of significant amounts of water. Amorphous material is not present, and with increasing petrologic type, increasing proportions of the originally opaque matrix appear translucent due to recrystallization; mineral grains have grown large enough to make up a significant fraction of the thickness of the thin section. Recrystallized matrix is less porous and contains less C than opaque matrix (*Huss et al.,* 1981). Furthermore, as the recrystallized matrix becomes more abundant, the remaining opaque matrix becomes coarser, less friable, and increasingly depleted in minute metallic Fe-Ni and sulfide

grains (*Huss et al.,* 1981). For example, matrix olivines in Chainpur (LL3.4) have begun to coalesce to form a mesh-like texture (*Nagahara,* 1984). By type 4, the matrix consists entirely of translucent to transparent crystals, although it can still be identified by grain size, morphology, and location. These changes are illustrated in Fig. 1.

Accompanying the textural changes are major changes in matrix mineralogy, composition, and mineral chemistry. As petrologic type increases, matrix olivine grains show less compositional spread, until by type ~3.8, they have largely equilibrated at the mean Fa content for the bulk meteorite (Fig. 2). With increasing petrologic type, plagioclase, chromite, and chlorapatite nucleate and grow, and minute sulfide and metallic Fe-Ni grains that are abundant in the matrix of type 3.0 ordinary chondrites coalesce into larger metal and sulfide grains (*Dodd et al.,* 1967; *Huss et al.,* 1981; *Grossman and Brearley,* 2005). Low in the metamorphic sequence, the Na, S, and Ni contents of the matrix decrease as alkalis enter chondrules, and sulfides and metal grains recrystallize (*Wood,* 1967; *Grossman and Brearley,* 2005). Above petrologic type ~3.5, matrix begins to show strong blue CL (*Sears et al.,* 1990) and the alkali content again rises, indicating that secondary feldspar grains have begun to grow (*Grossman and Brearley,* 2005).

The matrix of type 3 ordinary chondrites is host to a variety of presolar materials, including diamond, graphite, silicon carbide, oxides, deuterium-rich organic compounds, and crystalline and amorphous silicates (e.g., *Nittler,* 2003; *Mostefaoui et al.,* 2004). The abundances of presolar components correlate strongly with the petrologic type of the host meteorites (Fig. 3). Different presolar components have different susceptibilities to metamorphic breakdown. For example, presolar silicates and graphite have only been found in type 3.0–3.1, whereas diamond persists up to type 3.7–3.8 and the carrier of P1 noble gases (also known as Q gases) survives into type 4 and beyond (*Huss and Lewis,* 1995; *Huss et al.,* 1996; *Mostefaoui et al,* 2004).

2.1.3. Effects on silicate minerals in chondrules.

2.1.3.1. Mesostasis: Chondrule mesostasis in type 3 ordinary chondrites generally consists of feldspathic glass ± very small crystallites (<5 μm) and is highly susceptible to metamorphic alteration. Isotropic glass is common in low-FeO chondrules in type 3.00 Semarkona, but has mostly devitrified in related chondrules in type 3.6 Parnallee (*McCoy et al.,* 1991). *DeHart et al.* (1992) observed that the abundance of crystallites in the mesostasis also increases with metamorphic grade, again consistent with progressive devitrification.

The composition of chondrule mesostasis changes markedly during metamorphism. FeO increases and TiO_2 decreases in mesostasis in FeO-poor type I chondrules between types 3.0 and 3.6, whereas FeO and MnO decrease in mesostasis from FeO-rich type II chondrules along this sequence (*McCoy et al.,* 1991). In type I chondrules, the abundances of Na and K increase as these elements diffuse into the mesostasis and Ca is lost (*Sears et al.,* 1990; *Alexander et al.,* 2000; J. N. Grossman, unpublished data, 2005).
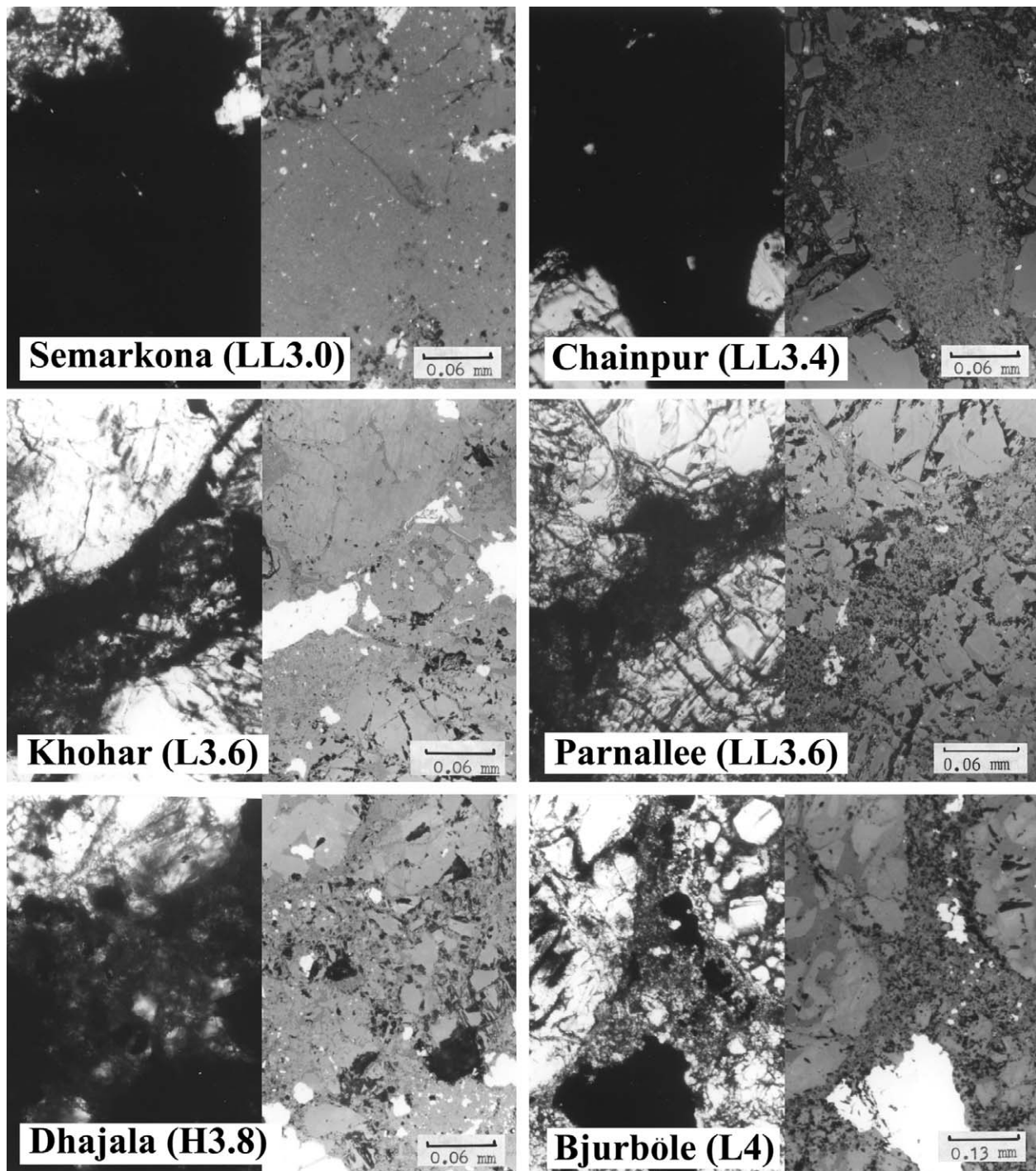
Fig. 1. Photomicrographs of the matrix in six chondrites. For each meteorite, the left image is in transmitted light and the right image is the same area in reflected light. In Semarkona (LL3.0), the matrix is opaque in thin section and consists of very fine-grained silicates, sulfides, and Fe-Ni metal. In Chainpur (LL3.4), the matrix is still largely opaque, but the matrix mineral grains are larger. In Khohar (L3.6) and Parnallee (LL3.6), the matrix is translucent in reflected light because the size of the mineral grains is approaching the thickness of the section. Sulfides and metal have coalesced into larger grains. In Dhajala (H3.8), most matrix minerals are now large enough to see in transmitted light. In Bjurbole (L4), the matrix is completely recrystallized and the grains are larger (note scale), although matrix can still be recognized by its grain size and location between chondrules.

The entry of alkalis is followed by crystallization of albitic feldspar by type ~3.4 (*Grossman and Brearley,* 2005). In the mesostasis of type II chondrules, crystalline albite is present even in type 3.00 Semarkona, but the abundance increases with petrologic type. Development of albite is responsible for the increase in blue CL shown by chondrules in type 3 ordinary chondrites as a function of metamorphic grade (see above) (*Grossman and Brearley,* 2005). As feld-
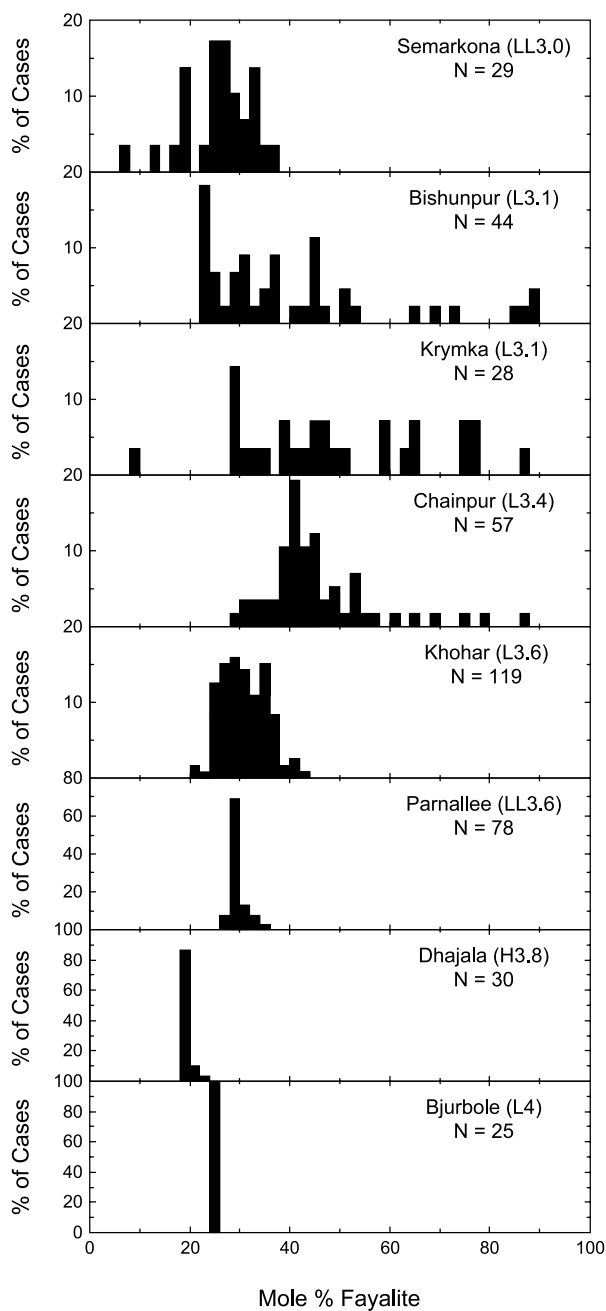
Fig. 2. Histograms showing fayalite contents of matrix olivine as a function of petrologic type. The distribution is widest in type 3.1 chondrites, and becomes systematically narrower with increasing petrologic type. By type 3.6 to 3.8, the matrix olivine has equilibrated at the mean fayalite value for the bulk meteorite. Chondrule olivine equilibrates by type 4. Data from *Huss et al.* (1981).

spar crystallizes from chondrule mesostasis during metamorphism, K/Na in residual glass rises to several times the solar ratio (*Grossman and Brearley,* 2005).

2.1.3.2. *Olivine:* Olivine compositional variability is a strong indicator of metamorphic grade (*Van Schmus and Wood,* 1967; *Dodd et al.,* 1967). Chondrule olivine from highly unequilibrated ordinary chondrites has a wide range of Fa contents (e.g., Fig. 1 of *Dodd et al.,* 1967). With in-

creasing petrologic type, the Fa content becomes increasingly uniform and converges on the value for equilibrated chondrites of the same group. The traditional measure of olivine heterogeneity (defined by *Dodd et al.,* 1967) is percent mean deviation (PMD, see notes for Table 1). Percent mean deviation remains high between types 3.0 and 3.4 (*Sears et al.,* 1980), but drops systematically as metamorphism proceeds from type 3.4 to type 4 (defined by PMD <5%). During this process, igneous zoning profiles in chondrule olivine are erased and FeO from the matrix diffuses into forsteritic chondrule olivine along grain boundaries and cracks (*McCoy et al.,* 1991). In a similar way, the MnO and P_2O_5 contents of olivine homogenize during metamorphism (*DeHart et al.,* 1992).

Although the PMD of chondrule olivine is not sensitive to metamorphic changes between types 3.0 and 3.4, there are profound changes in olivine chemistry within this range. Olivine in low-FeO chondrules begins to take up FeO by type 3.1, and by type 3.3 many type I chondrules contain significant FeO in olivine (*DeHart et al.,* 1992; *Scott et al.,* 1994). High CaO contents (>0.3 wt%) are common in olivine from types 3.0–3.1 chondrites, but by types 3.3–3.4 these concentrations occur less frequently, and by type 3.8 converge to near the equilibrated value of <0.05 wt%. Similar CaO losses occur in olivine from FeO-rich type II chondrules during metamorphism, although compositions with >0.2 wt% CaO are rare in these chondrules even in type 3.0. Like CaO, both TiO_2 and Al_2O_3 are enriched in some low-
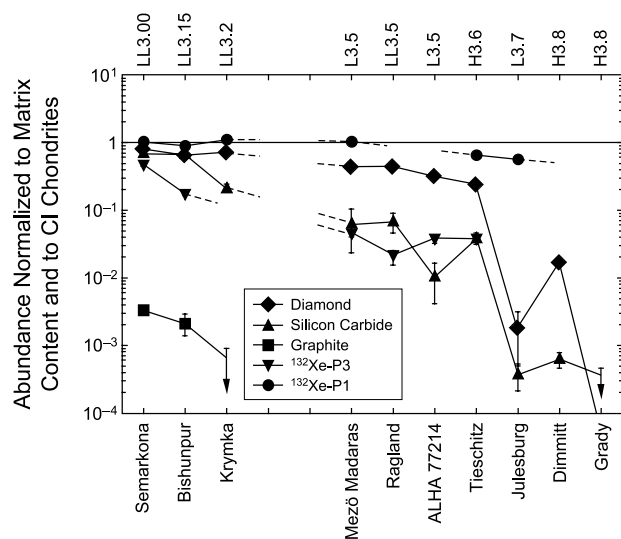
Fig. 3. Abundances of several presolar components found in primitive chondrites as a function of petrologic type of the host meteorites. The abundances have been normalized to vol% matrix (the grains are sited in the matrix) and are plotted as ratios to the abundances in CI chondrites (absolute abundances vary by several orders of magnitude). Although the absolute resistance to metamorphism varies dramatically among the plotted phases, all components decrease with increasing petrologic type. Most are effectively gone by type 3.8, where the matrix is almost completely recrystallized. Data from *Huss and Lewis* (1994, 1995) and *Huss et al.* (1996).

FeO chondrule olivines in type 3.0, but these compositions are lost during metamorphism (*DeHart et al.,* 1992; *Scott et al.,* 1994).

One of the most sensitive indicators of metamorphism in type 3 ordinary chondrites is the Cr_2O_3 content of olivine in type II chondrules. The Cr_2O_3 contents of these olivine grains decrease from ~0.5 wt% in type 3.0 chondrites to 0.15–0.2 wt% in type 3.2–3.3 to below detection limit in type 3.6–3.8 (*McCoy et al.,* 1991; *DeHart et al.,* 1992). *Grossman and Brearley* (2005) showed that in type 3.0–3.2 ordinary chondrites the distribution of Cr_2O_3 within FeO-rich olivine grains changes systematically and may be used to differentiate among the types. Experimental data confirm the extreme sensitivity of Cr_2O_3 in olivine to loss during heating (*Jones and Lofgren,* 1993).

2.1.3.3. *Pyroxene:* Pyroxene is relatively resistant to metamorphic alteration compared to other silicate minerals in chondrules. Whereas olivine begins equilibrating in the lowest petrologic types, and the PMD of its Fa content begins to decrease by type 3.4, the PMD of the ferrosilite (Fs) content of low-Ca pyroxene remains high until at least type 3.6–3.8 and is still relatively high into type 4 (*Dodd et al.,* 1967). During metamorphism of FeO-poor type I chondrules, FeO and MnO increase and Cr_2O_3 and Al_2O_3 decrease in low-Ca pyroxene (*McCoy et al.,* 1991). *DeHart et al.* (1992) observed that the CaO content of high-Ca pyroxene decreases somewhat with increasing petrologic type.

2.1.4. *Effects on nonsilicate minerals.* In type 3.0 ordinary chondrites, P, Si, and Cr occur in solid solution in some metallic Fe-Ni grains in type I chondrules (*Zanda et al.,* 1994); phosphides and silicides may also be present as inclusions in metal. By petrologic type 3.1, these elements leave the metal, reacting with atomic species from elsewhere in the meteorite (e.g., Ca, Fe, O, Cl). Even in type 3.00 Semarkona, Cr has been oxidized from metal grains in many type I chondrules. In some metal grains from type 3.15 Bishunpur, Na and Fe phosphates, chromite, and silica are present as inclusions; reduced P-, Si-, and Cr-bearing phases are absent (B. Zanda, personal communication, 2003). At or above type 3.1, Ca-phosphate becomes the dominant P-rich phase associated with chondrule metal, and phosphates form at the edges of metal grains (*Rambaldi and Wasson,* 1981; B. Zanda, personal communication, 2003), forming mantles (*Rubin and Grossman,* 1985). Large phosphates >20 μm in diameter found in the matrix of Parnallee (LL3.6), Bremervörde (H/L3.9), and Dhajala (H3.8) are presumably of metamorphic origin (*Huss et al.,* 1981).

Kamacite in type 3.0 ordinary chondrites is heterogeneous with respect to Ni and Co (e.g., Fig. 163 of *Brearley and Jones,* 1998). With increasing metamorphism, the concentrations of Ni and Co become more uniform, and the mean concentrations tend to increase (*Rubin,* 1990). Nickel in taenite grains is unzoned in type 3.0–3.1 ordinary chondrites, whereas zoned taenite is present at type 3.4 and above (*Wood,* 1967; *Afiattalab and Wasson,* 1980). During metamorphism, Ni diffuses out of kamacite and into taenite. With cooling, diffusion becomes more sluggish. At the kamacite-taenite interface, Ni becomes depleted at the edges

of kamacite grains (the so-called Agrell dip) and enriched at the edges of taenite grains, leaving "M-shaped" Ni profiles in the taenite. These frozen-in diffusion profiles have been used to estimate cooling rates of chondrites (e.g., *Wood,* 1967; *Willis and Goldstein,* 1981).

In the most primitive type 3 ordinary chondrites, much of the low-Ni metal has been replaced by a complex mixture of carbides, magnetite, Ni-rich metal, and Ni-rich sulfides (*Huss,* 1979; *Taylor et al.,* 1981). These assemblages occur as large millimeter-sized masses between chondrules in Semarkona (LL3.00) and Ngawi (LL3.0–3.6 breccia), and they probably originated through hydrothermal alteration of metallic iron by a C-O-H fluid on the parent body (*Krot et al.,* 1997). Less complex but similar magnetite-sulfide assemblages surround chondrules, particularly in Semarkona. These assemblages exhibit structures consistent with fluid deposition and grade into the matrix; they appear to have formed in place during fluid-assisted metamorphism (*Huss,* 1979).

2.1.5. *Bulk effects.*   The bulk compositions of ordinary chondrites are largely unaffected by metamorphism (e.g., *Kallemeyn et al.,* 1989). However, the abundances of some volatile and mobile elements decrease with increasing petrologic type (Table 1). Much of this variation occurs among the type 3 ordinary chondrites, although some parameters continue to decrease right through type 6. Bulk contents of C, H_2O, and primordial (=P1 or Q) noble gases decrease with increasing petrologic type in ordinary chondrites (Table 1) (*Van Schmus and Wood,* 1967; *Zähringer,* 1968; *Alaerts et al.,* 1979). Whereas water is truly mobile, much of the C in type 3 ordinary chondrites is in relatively refractory organic compounds, some of which are the noble-gas carriers (e.g., *Huss et al.,* 1996). These compounds are easily oxidized to CO and CO_2, releasing the noble gases and producing the observed correlation between C and noble gases. Among true volatile elements, the Cs, Cd, Bi, Tl, and In contents of type 4–6 chondrites are lower by 1–2 orders of magnitude than those in type 3 [first shown for In by *Tandon and Wasson* (1968); see reviews by *Dodd* (1969) and *Lipschutz and Woolum* (1988)].

2.2. CO3 Chondrites

McSween (1977a) presented the first strong case that CO3 chondrites represent a metamorphic sequence. The CO3 chondrites are now subdivided using a scheme analogous to that of type 3 ordinary chondrites [3.0–3.7, *Scott and Jones* (1990); 3.0–3.8, *Chizmadia et al.* (2002); or 3.0–3.9, *Sears et al.* (1991a)]. In the following discussions, we use the classification of *Chizmadia et al.* (2002) because it seems to correlate better with that of type 3 ordinary chondrites. This system adds 0.1 to the classifications of *Scott and Jones* (1990) for all CO3 chondrites at or above type 3.1.

2.2.1. *Matrix.*   The matrix of CO3 chondrites changes markedly during metamorphism. The matrix of Allan Hills (ALH) A77307 (CO3.0) is highly unequilibrated and consists of an amorphous silicate component, olivine, pyroxene, magnetite, kamacite, pentlandite, pyrrhotite, anhydrite,

and disordered mixed-layer phyllosilicates (*Brearley,* 1993). There are two populations of olivine and pyroxene in ALH A77307 matrix. One consists submicrometer-sized grains of nearly pure forsterite and enstatite grains that are probably primary. A more-abundant type of poorly crystalline olivine has compositions ranging from Fa_{18} to Fa_{72} and is probably secondary (*Brearley,* 1993). The matrix of ALH A77307 also contains relatively high abundances of presolar grains, including presolar silicates (*Huss et al.,* 2003; *Kobayashi et al.,* 2005). Matrix in type 3.1–3.8 CO chondrites apparently does not contain tiny forsterite and enstatite grains and is dominated by fine-grained FeO-rich olivine (*Brearley,* 1995). With increasing petrologic type, the range of olivine compositions decreases (*Brearley and Jones,* 1998), and the mean Fa content of matrix Fe-rich olivine decreases systematically from $\sim Fa_{66-68}$ in ALH A77307 (CO3.0) to $\sim Fa_{32}$ in Warrenton (CO3.7) (*Scott and Jones,* 1990, and references therein). Abundances of presolar grains also decrease systematically with increasing petrologic type (*Huss,* 1990; *Huss et al.,* 2003). Matrix texture changes only slightly with increasing petrologic type, appearing somewhat turbid in Warrenton (CO3.7) and Isna (CO3.8) (*McSween,* 1977a) rather than opaque as in lower types.

Water played a role in the alteration history of some CO3 matrix. Allan Hills A77307 contains phyllosilicates and anhydrite that were probably produced *in situ,* although they might be weathering products from Antarctica (*Brearley,* 1993). The matrix of Lancé (CO3.4), a witnessed fall, also contains phyllosilicates that partially replace matrix olivine, but matrix in Kainsaz (CO3.2) and Warrenton (CO3.7) apparently does not contain phyllosilicates (*Keller and Buseck,* 1990).

2.2.2. Chondrules, calcium-aluminum-rich inclusions, and amoeboid olivine inclusions.   Type IA chondrules in CO chondrites show systematic increases in the Fa content of olivine and the Fs content of low-Ca pyroxene and a systematic decrease in the CaO content of olivine from type 3.0 to type 3.8 (*Scott and Jones,* 1990). Type II chondrules show a similar trend for CaO content, but not for mean Fa content because the olivine in type II chondrules started out close to the equilibrium Fa content for CO3 chondrites. These changes are best understood in terms of diffusional exchange between matrix and chondrules, with equilibration approached, but not reached, by type CO3.8 (e.g., *Scott and Jones,* 1990).

Chondrule mesostases show increasing degrees of alteration that correlate with petrologic type. *Itoh and Tomeoka* (2003) found that chondrules in Yamato (Y) 81020 (CO3.0) have unaltered mesostases with little nepheline. In contrast, 60% of the chondrules in CO3.2 chondrites and >90% of the chondrules in CO3.3–3.5 chondrites have minor to moderate degrees of mesostasis alteration and abundant nepheline. The chondrule mesostases in Warrenton (CO3.7) have been nearly completely replaced by nepheline or nepheline-rich aggregates.

Calcium-aluminum-rich inclusions (CAIs) have experienced considerable secondary alteration, both before and after accretion (*Russell et al.,* 1998). Probable metamorphic alteration on the parent body can be identified by correlations between CAI characteristics and petrologic type. For example, melilite-rich inclusions are abundant in CO3.0–3.4 meteorites, rare in CO3.5 meteorites, and absent in CO3.6–3.8. Melilite in CAIs is probably replaced by feldspathoids, pyroxene, and Fe-rich spinel. Spinel in melilite-rich and coarse-grained spinel-pyroxene inclusions becomes more Fe-rich, with development of nearly homogenous hercynitic spinel (~50–60 mol% hercynite) in types >3.5. Perovskite has been converted to ilmenite in types >3.5 (*Russell et al.,* 1998).

Amoeboid olivine inclusions (AOIs) (also called amoeboid olivine aggregates, AOAs) in CO3 chondrites are sensitive to parent-body aqueous alteration and thermal metamorphism (*Rubin,* 1998; *Chizmadia et al.,* 2002). Between types 3.0 and 3.2, forsterite grains in AOIs acquire thin ferroan olivine (Fa_{60-75}) rims. By type 3.4–3.5, the fayalitic rims have thickened, and the olivine compositional distributions of individual AOIs have broadened and become bimodal. At type 3.6–3.7, the compositions of AOI olivine become unimodal at $\sim Fa_{65}$ although there is still a low-Fe tail. The high-Fe peaks are rather broad, extending from Fa_{50-55} to Fa_{68-70}. By type 3.8, the forsteritic tails disappear and only ferroan olivine remains in a relatively narrow peak at $\sim Fa_{65}$. In addition to changes in FeO/(FeO + MgO), the abundances and variability of Mn, Cr, and Ca in AOI olivine grains decrease as equilibrium is approached (*Chizmadia,* 2000).

Although matrix and AOIs in CO3.8 meteorites each approach equilibration, they are not equilibrated with each other (*Methot et al.,* 1975; *Scott and Jones,* 1990; *Chizmadia et al.,* 2002). In addition, chondrule silicates are far from equilibrated (*Scott and Jones,* 1990), showing olivine and pyroxene distributions similar to type ≤3.5 ordinary chondrites (cf. *Dodd et al.,* 1967; *Huss et al.,* 1981). Thus, even the highest-grade CO3 meteorites in our collections are not equilibrated chondrites.

2.2.3. Metal.   Kamacite grains in CO3.0 chondrites contain high concentrations of Cr, P, and Si, as do metal grains from the least-metamorphosed LL chondrites (see above). Kamacite shows systematic increases in the mean concentrations of Ni and Co from CO3.0 to CO3.8, while Cr content (and presumably P and Si content) in metal decreases (*McSween,* 1977a; *Scott and Jones,* 1990).

2.3. CV3 Chondrites

The CV3 chondrites and their constituents have been heavily affected by secondary processes, including alkali-halogen-Fe metasomatism, aqueous alteration, thermal metamorphism, and shock metamorphism (e.g., *Krot et al.,* 1995). As a result, attempts to divide CV3 chondrites into petrologic subtypes (e.g., *Guimon et al.,* 1995) have not been particularly successful (e.g., *Krot et al.,* 1995). CV3 chondrites have been divided into oxidized and reduced subgroups, and the oxidized subgroup has been subdivided into $CV3_{oxA}$ and $CV3_{oxB}$ largely based on the style of secondary-alteration features (*McSween,* 1977b; *Weisberg et al.,*

1997). In this section, we discuss the secondary features of each subgroup of CV3 chondrites that have been attributed to parent-body metamorphism.

2.3.1. $CV3_{oxB}$ chondrites. Oxidized CV3 chondrites of the Bali type (Bali, Kaba, portions of Mokoia, Grosnaja, and ALH 85006) have experienced significant secondary processing (*Krot et al.,* 1995, 1998a). In Kaba, alteration of chondrule mesostasis (*Keller and Buseck,* 1990) and associated redistribution of Ca, Si, Al, Mg, Fe, Mn, and Na (*Krot et al.,* 1998a) is best understood in terms of aqueous alteration on the parent body. A similar origin is likely for phyllosilicate, tetrataenite, awaruite, and pentlandite in the matrix of Kaba and Mokoia (*Keller and Buseck,* 1990; *Krot et al.,* 1995). Other features in Kaba, including Fe-rich halos around some opaque nodules and veins of fayalitic olivine within forsterite grains, are more likely due to high-temperature processing (e.g., *Hua et al.,* 2005). Similar features in other CV3 chondrites have been linked to processing prior to the final accretion of the parent body (*Peck and Wood,* 1987; *Krot et al.,* 1995). However, the decreasing spread of matrix-olivine Fa compositions going from Fa_0–Fa_{100} in Kaba to Fa_{10}–Fa_{75} in Mokoia to Fa_{35}–Fa_{55} in Grosnaja appears to be a metamorphic sequence (e.g., *Krot et al.,* 1995).

2.3.2. $CV3_{oxA}$ chondrites. Oxidized CV3 chondrites of the Allende type (e.g., Allende, Axtell, Lewis Cliff 86006, and ALH A81258) have experienced considerable alkali-halogen-Fe metasomatism (*Krot et al.,* 1995). Metasomatic effects include replacement of primary minerals in CAIs and their Wark-Lovering rims by secondary nepheline, sodalite, grossular, anorthite, hedenbergite, and other phases, and entry of Fe into spinel. Metasomatism of chondrules in Allende and Axtell has resulted in replacement of mesostasis with secondary minerals (*Kimura and Ikeda,* 1995; *Srinivasan et al.,* 2000), enrichment of olivine and pyroxene in Fe, and replacement of low-Ca pyroxene by fayalitic olivine (*Housley and Cirlin,* 1983; *Krot et al.,* 1995; *Srinivasan et al.,* 2000). Many coarse-grained igneous rims around chondrules contain secondary nepheline and sodalite (*Rubin,* 1984). Matrix has also been extensively affected by alkali-halogen-Fe metasomatism. The site of this metasomatism is still unknown. Earlier workers favored alteration prior to accretion (*Peck and Wood,* 1987; *Palme and Wark,* 1988; *Kimura and Ikeda,* 1995), but in a series of papers, Krot and co-workers have made a case for parent-body alteration (*Krot et al.,* 1995, 1998a, 1998b).

Thermal metamorphism also affected $CV3_{oxA}$ chondrites. In Axtell and Allende, matrix olivine has a restricted range of compositions (~$Fa_{40–50}$), suggesting a higher metamorphic grade than in other oxidized and reduced CV3s (e.g., *Krot et al.,* 1995). Abundances of presolar grains suggest that Allende is somewhat more metamorphosed than Axtell and that both are significantly more metamorphosed than Mokoia, Leoville, and Vigarano (*Huss et al.,* 2003). This sequence is consistent with that derived from olivine data, but is inconsistent with the one based on TL sensitivity (*Guimon et al.,* 1995).

2.3.3. $CV3_{red}$ chondrites. In many ways, the $CV3_{red}$ chondrites (Leoville, Efremovka, Vigarano, Arch) show the least evidence of secondary processing. Reduced CV3s have primary metal and troilite as their main opaque phases (*Krot et al.,* 1995, 1998a). Their CAIs show little evidence for alkali-halogen-Fe metasomatism (*Krot et al.,* 1995), and secondary phases are rare or absent from their matrix (e.g., *Krot et al.,* 1998a). However, the presence in matrix of abundant fayalitic olivine with a restricted range of composition and absence of amorphous material and forsterites that are common in matrix of the most primitive chondrites suggest that even the least-altered $CV3_{red}$ chondrites have experienced some alteration (*Krot et al.,* 1998a). Abundances of presolar diamond and SiC indicate that Leoville is less metamorphosed than Vigarano (*Huss and Lewis,* 1995), consistent with the order obtained from TL sensitivity (*Guimon et al.,* 1995).

2.3.4. Comparing $CV3_{red}$, $CV3_{oxB}$, and $CV3_{oxA}$ chondrites. The three subclasses of CV3 chondrites have experienced different levels of aqueous alteration, metasomatism, and thermal metamorphism. The $CV3_{oxB}$ meteorites experienced significant aqueous processing, while $CV3_{oxA}$ meteorites primarily show evidence of metasomatism; few meteorites show evidence of both, perhaps implying that metasomatism actually represents aqueous alteration followed quickly by thermal metamorphism. The $CV3_{red}$ meteorites show little evidence of either aqueous alteration or metasomatism (e.g., *Krot et al.,* 1995). Spreads in matrix olivine compositions indicate that Kaba ($CV3_{oxA}$) is among the least metamorphosed, followed by Leoville ($CV3_{red}$) and Mokoia ($CV3_{oxA}$), followed in turn by Vigarano ($CV3_{red}$) and Grosnaja ($CV3_{oxB}$), and then by Axtell and Allende (both $CV3_{oxA}$) (Fig. 8 of *Krot et al.,* 1995; Fig. 10.2.6 of *Scott et al.,* 1988). Abundances of presolar grains imply that Leoville is slightly less metamorphosed than Mokoia, followed in turn by Vigarano, Axtell, and Allende (*Huss et al.,* 2003). Raman spectroscopy of organic material indicates that Leoville is the least altered, followed by Vigarano ≈ Kaba ≈ Efremovka < Grosnaja < Mokoia < Axtell < Allende (*Bonal et al.,* 2004). These studies give a similar order, but this order is not consistent with that inferred from TL sensitivity (*Guimon et al.,* 1995), except perhaps among $CV3_{red}$ meteorites.

2.4. Other Chondrite Groups

2.4.1. Carbonaceous chondrites. Most other carbonaceous chondrite groups consist of nearly unmetamorphosed meteorites. There is little evidence that CH, CB, and CR chondrites have experienced any metamorphic heating (*Weisberg et al.,* 2001; *Krot et al.,* 2002). In most CI and CM chondrites, the effects of severe aqueous alteration obscure any metamorphic history they might have had. However, a small group of CI and CM chondrites do show metamorphic effects (*Zolensky et al.,* 2005). *Tonui et al.* (2001) describe blurring of chondrule boundaries and other effects of significant heating in some of these chondrites, implying metamorphic conditions above type 3. However, highly unequilibrated olivine compositions seem to be more consistent with petrologic types below 3.2 (*Grossman et al.,*

2005). The CK group has metamorphosed and unmetamorphosed members (*Kallemeyn et al.,* 1991), but CK and Kakangari-like chondrites have too few type 3 representatives to permit systematic studies of their metamorphic properties. Further study is clearly required to deduce the thermal histories of these meteorites.

2.4.2. Enstatite chondrites.   Type 3 members are well described in both the EH and EL groups. EH3 and EL3 chondrites are texturally similar, having well-delineated chondrules and containing minor olivine (<1% to 5% by volume), but EL chondrites have larger chondrules on average than EH chondrites and their mineral chemistries differ somewhat (*Binns,* 1967; *Prinz et al.,* 1984; *Rubin et al.,* 1997). The matrix in type 3 enstatite chondrites is not well characterized. It is typically not opaque, as it is in type 3 ordinary chondrites, but is fine-grained and recognizable by its grain size, morphology, and location. The matrix of EH3 chondrites (and presumably EL3 chondrites, although no data are yet available) acquired abundances of presolar diamond and SiC similar to other chondrite classes (*Huss and Lewis,* 1995).

In general, we know little about the metamorphic history of type 3 enstatite chondrites. Although they display considerable mineralogical variation, they cannot easily be put into a metamorphic sequence because they have had complex thermal and shock histories compared to ordinary and carbonaceous chondrites (*Zhang et al.,* 1995).

2.4.3. R chondrites.   Rumuruti (R) chondrites resemble ordinary chondrites in many ways: They have large chondrules, $\Delta^{17}O > 0$, and similar chondrule types. They show a similar range of petrologic types as well, although most R3 chondrites have experienced metamorphism equivalent to at least type 3.6 in ordinary chondrites (*Rubin and Kallemeyn,* 1989; *Bischoff et al.,* 1994). The only highly unequilibrated material described in the literature consists of clasts of petrologic type <3.5, possibly as low as 3.2, in some R chondrite breccias (*Bischoff,* 2000). Matrix in the R3.8 chondrites shows evidence of recrystallization; it is a low-porosity, translucent material that consists primarily of olivine accompanied by minor 2–3-μm pyroxene grains micrometer-sized sulfide grains, and, in some cases, 10-μm patches of plagioclase (*Kallemeyn et al.,* 1996). Again, little is known about the metamorphic effects in R3 chondrites, although matrix material and chondrule olivine clearly underwent Fe-Mg exchange similar to that in ordinary chondrites.

3. HIGHER-TEMPERATURE EFFECTS (TYPES 4–6)

Metamorphic changes in type 4–6 chondrites have been significant, but many of the criteria used to classify type 3.00–3.9 chondrites do not help to classify these "equilibrated" chondrites. Criteria used to classify type 4–6 ordinary chondrites are summarized in Table 1. Because the most useful ones tend to be somewhat subjective, the boundaries between types 4, 5, and 6 are rather poorly defined. Classification can also be difficult if a meteorite is a breccia

containing material of different petrographic types. In such a meteorite, the current assemblage has never been heated above the temperature experienced by the lowest-grade material.

3.1. Ordinary Chondrites

3.1.1. Textural integration.   Textural differences between type 3 chondrites and type 4–6 chondrites are significant and well documented (*Dodd et al.,* 1967; *Van Schmus and Wood,* 1967). Textural integration of matrix, chondrules, chondrule fragments, and inclusions proceeds up the metamorphic scale (Fig. 4), and is observable in chondrites of high petrologic type 3 and above. The opaque, fine-grained matrix found in primitive type 3 ordinary chondrites has completely recrystallized by type 4, but is still recognizable as matrix. By type 5, matrix is no longer recognizable, and textural integration between chondrules and matrix has begun. In type 6, small chondrules have lost their identity and only large chondrules are readily recognizable (Fig. 4). The mean modal abundance of recognizable chondrules decreases from 65–75 vol% in H3 chondrites (Table 1 of *Rubin,* 2000) to 22 vol% in H5 and 11 vol% in H6 (Table 2 of *Rubin et al.,* 2001).

3.1.2. Grain growth and appearance of new phases. Coarse-grained plagioclase is essentially absent from type 3 ordinary chondrites, except for anorthitic phenocrysts in rare Al-rich chondrules (e.g., *Russell et al.,* 2000). Small primary plagioclase grains also occur in coarse-grained, igneous rims around chondrules (*Rubin,* 1984). The clear, Na- and Al-rich chondrule mesostasis observed in type 3 chondrules has begun to devitrify in high type 3s, as albitic plagioclase nucleates and begins to grow. By type 4, chondrules have turbid mesostasis. Type 5 ordinary chondrites contain mainly microcrystalline (~2–10 μm) plagioclase grains, whereas type 6s contain abundant plagioclase grains ≥50 μm in size (e.g., *Van Schmus and Wood,* 1967).

Diopside occurs as small, commonly skeletal, crystallites in the mesostases of some chondrules in type 3 ordinary chondrites, but it is rare to absent in the fine-grained silicate matrix. Diopside is typically of submicrometer size in type 4s; it occurs as 2–5-μm grains in type 5s and as coarser grains (up to tens of micrometers) in type 6s.

Phosphate minerals and chromite occur as tiny grains (<5–10 μm) in type II chondrules, and nucleate as submicrometer secondary minerals in type I chondrules in the earliest stages of metamorphism (*Grossman and Brearley,* 2005). By type 5 and 6, grains of merrillite and chlorapatite have grown to tens of micrometers in size (*Van Schmus and Ribbe,* 1969). Chromite grains in unshocked type 4–6 chondrites can be as large as 200 μm (*Rubin,* 2003). Metallic Fe-Ni and troilite coarsen significantly between types 3 and 6. For example, metal and troilite in H3.4 Sharps have mean particle sizes of ~65 μm and ~30 μm, respectively (*Benoit et al.,* 1998), whereas these phases have grown to ~120 μm and ~80 μm, respectively, in H5 and 6 chondrites (*Rubin et al.,* 2001). By type 6, many metal grains are no longer
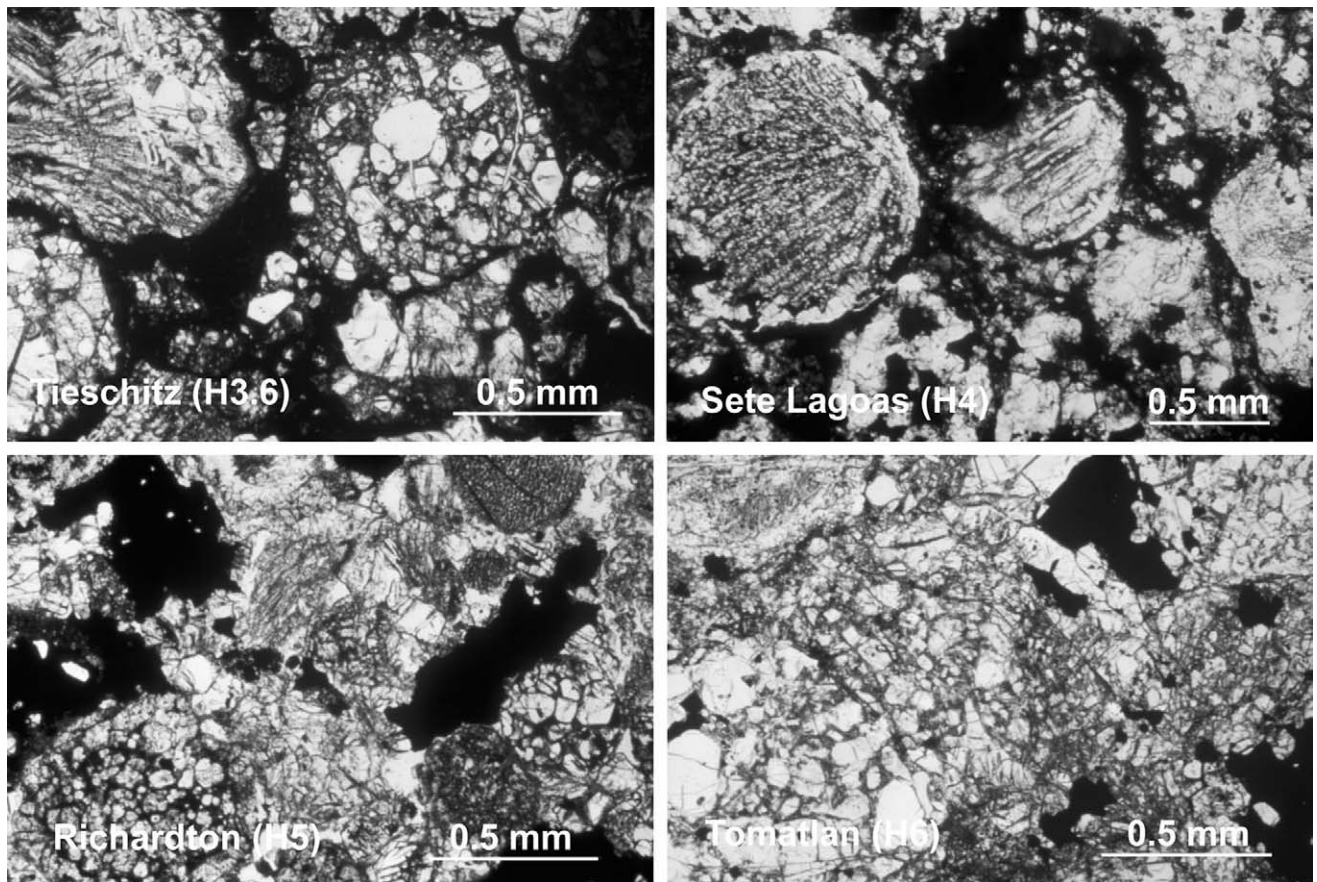
Fig. 4. Transmitted-light photomicrographs of representatives of type 3, 4, 5, and 6. Note the clearly defined chondrules and black, opaque matrix in Tieschitz (H/L3.6), the well-defined chondrules and recrystallized matrix in Sete Lagoas (H4), the integration of the chondrules with surrounding material and large metal grains in Richardton (H5), and the almost complete lack of identifiable chondrules in Tomatlan (H6). The black phases in the H4, H5, and H6 chondrites are metal and sulfide grains.

relatively compact, but have taken on irregular shapes defined by surrounding mafic-silicate grains (*Dodd,* 1969).

3.1.3. Phase transformation. Low-calcium clinopyroxene exhibiting polysynthetic twinning and inclined extinction commonly occurs as phenocrysts in chondrules in type 3 and 4 ordinary chondrites (e.g., Fig. 4.5 of *Dodd,* 1981). Low-calcium clinopyroxene transforms to orthopyroxene at ~630°C (*Boyd and England,* 1965) and thus is largely absent in types 5 and 6 (*Van Schmus and Wood,* 1967). However, low-Ca clinopyroxene can form by shock heating and quenching in chondrites of any petrologic type [stage ≥S3 (*Stöffler et al.,* 1991)].

3.1.4. Changes in mineral compositions. Many of the most striking compositional changes occur in type 3 chondrites as major silicate phases equilibrate. Olivine is equilibrated by type 4, but pyroxene equilibration is not completed until type 5 (*Van Schmus and Wood,* 1967; *Dodd et al.,* 1967). In the most metamorphosed members of type 6, classified by some workers as type 7, the CaO content of low-Ca pyroxene may be somewhat higher (>1 wt%) than in members that have experienced lower peak temperatures (*Dodd et al.,* 1975; *Mittlefehldt and Lindstrom,* 2001).

Metal grains do not equilibrate during metamorphism in ordinary chondrites due to sluggish diffusion. Instead, taenite grains exhibit a characteristic "M-shaped" Ni profile. These frozen-in diffusion profiles provide one means of estimating cooling rates of chondrites (e.g., *Wood,* 1967; *Willis and Goldstein,* 1981).

3.2. Carbonaceous Chondrites

3.2.1. CK chondrites. The CK chondrites are the only carbonaceous chondrites that exhibit the full range of petrologic types, CK3–CK6. *Kallemeyn et al.* (1991) described a number of metamorphic effects in CK chondrites that are analogous to those of ordinary chondrites. Homogeneity of olivine composition increases from type 3 to types 4–6. The mean diameter of plagioclase grains increases from CK3, where plagioclase is absent or microcrystalline, to CK4, where grains are <4 μm, to CK5 (4–50 μm) to CK6 (≥50 μm). Primary glass is found only in CK3 chondrules. Chondrule borders are sharply delineated in CK3, well defined in CK4, readily discernable in CK5, and poorly defined in CK6. The mean grain size of interchondrule mate-

rial coarsens from CK3 (≤0.1–10 μm) to CK4 (5–50 μm) to CK5 (50–200 μm) to CK6 (50–300 μm). This parameter is the most diagnostic feature of petrologic type in CK chondrites.

3.2.2. Other metamorphosed carbonaceous chondrites. Coolidge and Loongana 001 constitute a distinct grouplet of carbonaceous chondrites (*Kallemeyn and Rubin,* 1995). They have relatively uniform olivine and heterogeneous low-Ca pyroxene compositional distributions, characteristic of petrologic types 3.8 to 4. Several other metamorphosed carbonaceous chondrites have been described [e.g., Mulga (west)] but they are not yet sufficiently well characterized to determine if they are CK chondrites, members of the Coolidge-Loongana-001 subgroup, ungrouped individuals, or members of new grouplets.

3.3. Enstatite Chondrites

Enstatite chondrites comprise two distinct groups, EH and EL, that formed under highly reducing conditions (e.g., *Sears et al.,* 1982b). Both groups include meteorites from petrologic types 3–6. As in ordinary and carbonaceous chondrites, the texture and mineralogy of EH and EL chondrites change during progressive thermal metamorphism. Chondrules are sharply defined in type 3, well-defined in type 4, readily delineated in type 5, and poorly defined, recrystallized, or, in some cases, absent in type 6. Low-Ca pyroxene exhibits significant compositional heterogeneity in type 3 (Fs_0 to Fs_{35}), minor heterogeneity in type 4, and uniformity in types 5 and 6. Monoclinic low-Ca pyroxene is predominant in type 3 enstatite chondrites, abundant in type 4, and essentially absent in types 5 and 6 (which instead contain orthopyroxene). Crystalline plagioclase is absent or fine-grained in type 3, coarser-grained (5–50 μm) in types 4 and 5, and very coarse-grained (≥50 μm) in type 6. Olivine decreases in abundance from 0.2 to 5 vol% in E3 chondrites to 0 to 1 vol% in E4; olivine is absent in E5 and E6. The nickel silicide, perryite $[(Ni,Fe)_5(Si,P)_2]$, is relatively abundant in EH3 chondrites (e.g., perryite constitutes 15% of the total opaque phases in Kota-Kota), but it is rare in EH4 and EH5 chondrites (e.g., *Reed,* 1968; *Prinz et al.,* 1984). As perryite disappears during metamorphism, its elemental constituents are partitioned mainly into kamacite.

The abundances of presolar diamond and SiC also correlate with petrologic type in EH chondrites. Unlike in other chondrite groups, these phases persist in EH4 and perhaps even EH5 chondrites, probably because the reduced compositions of the host meteorites allow the presolar grains to survive to higher metamorphic temperatures without undergoing oxidation (*Huss and Lewis,* 1995).

Enstatite chondrites also exhibit properties that, although they correlate with petrologic type, cannot be explained by thermal metamorphism. For example, EH5 and EL6 chondrites contain high abundances of a "subsolar" noble gas component in their silicates that is either absent or present in only very low abundance in EH3 and EH4 chondrites (*Crabb and Anders,* 1981, 1982). These gases have a less-severe elemental fractionation relative to solar-system abundances than do planetary gases, and neither the fractionation nor the abundances can be produced by thermal metamorphism of more primitive material. This implies that these gases were acquired prior to accretion, which presents an interesting problem for models attempting to explain the range of properties of EH or EL chondrites strictly in terms of metamorphism.

3.4. R Chondrites

Many R chondrites are petrologic type 3.8–4 (e.g., Rumuruti, Carlisle Lakes, NWA 2198), and some are regolith breccias containing clasts with a diverse array of petrologic types (e.g., PCA 91002, R3.8–6) (*Kallemeyn et al.,* 1996). The R5 and R6 clasts are moderately to highly recrystallized, and matrix material is not recognizable. Highly recrystallized chondrules occur in R5 clasts, but discernable chondrules are absent in R6 clasts. A few R5 chondrites have been described (including the possibly paired NWA 830, 1585, 1668, 3098, and the unrelated find Sahara 99527). No individual R6 chondrites have been described.

4. TEMPERATURES OF METAMORPHISM

Two types of metamorphic temperatures are discussed in the literature. Peak metamorphic temperature, the highest temperature reached during metamorphism, is typically estimated from phase changes or reactions that occur at specific temperatures. Peak temperatures are particularly relevant for unequilibrated chondrites. Equilibration temperatures are determined from coexisting mineral phases and typically reflect the lowest temperature during the cooling of the system at which minerals remained in diffusive equilibrium. To accurately reflect metamorphism, the temperature must have been high enough to erase partitioning established during chondrule formation or other earlier high-temperature events. Temperatures given for equilibrated chondrites are typically equilibration temperatures, and in some cases they may approach the peak temperature. Typically, pressure is not an issue because metamorphism in chondrites probably occurred at pressures of ≤1 kb (e.g., *Dodd,* 1981; *McSween and Patchen,* 1989).

4.1. Ordinary Chondrites

Dodd (1981) estimated that type 3 ordinary chondrites reached temperatures of 400°–600°C, but these temperatures are clearly too high for the lowest petrologic types. *Alexander et al.* (1989a) set an upper limit of ~260°C for the alteration temperature of Semarkona (LL3.00) based on matrix clay mineralogy. *Rambaldi and Wasson* (1981) used the Ni content of matrix metal to estimate a metamorphic temperature of 300°–350°C for Bishunpur (LL3.15). *Brearley* (1990) used a thermometer based on the degree of or-

dering of poorly graphitized C (*Reitmeijer and MacKinnon*, 1985) to derive temperatures of 350°–400°C for type 3.4–3.6 chondrites. On the other hand, *Sears et al.* (1991b) inferred temperatures of 500°–600°C for type 3.5 chondrites based on the order/disorder transition of feldspar. *Wlotzka* (1985, 1987) used the Cr-spinel/olivine thermometer to estimate equilibration temperatures of 600°–700°C for Dhajala (H3.8), Study Butte (H3.7), and Clovis (no. 1) (H3.7), whereas *McCoy et al.* (1991) estimated peak temperatures for type 3.7–3.8 ordinary chondrites of 525°–600°C. *Huss and Lewis* (1994) used these data and the amounts of P3 noble gases in presolar diamonds to construct a temperature scale for type 3 ordinary chondrites (and other primitive meteorites) ranging from ~200°C for Semarkona (LL3.00) to ~600°C for Parnallee (LL3.6). This temperature scale is a smooth (but probably not linear) function of petrologic type within a meteorite class.

Type 4–6 ordinary chondrites have reached higher temperatures than type 3s, with an upper limit defined by the onset of melting at ~950°C (*Dodd*, 1981). Some partially melted chondrites (i.e., primitive achondrites) may have reached as much as 1150°C (*McSween and Patchen*, 1989). Equilibration temperatures for type 6 chondrites based on Ca-Mg partitioning between coexisting high-Ca pyroxenes are systematically 50°–150°C higher than those based on similar partitioning in low-Ca pyroxene (*McSween and Patchen*, 1989; *Harvey et al.*, 1993) and ~200°C higher than those based on olivine-spinel equilibrium (*Kessel et al.*, 2002). These temperatures reflect differences in closure temperatures for the three systems (*Kessel et al.*, 2002). High-Ca pyroxene probably gives the best estimate for peak metamorphic temperature in type 6 chondrites: 900°–960°C for LL6, 850°–950°C for L6, and 800°–950°C for H6 (*McSween and Patchen*, 1989; *Harvey et al.*, 1993). Temperatures for LL6 chondrites seem to be the best determined. Several studies have shown evidence for decreasing peak temperature from LL6 to L6 to H6 (*Dodd*, 1981; *Olsen and Bunch*, 1984; *Harvey et al.*, 1993), but equilibration temperatures reflect cooling rate as well as peak temperature. Temperatures for types 4 and 5 chondrites are hard to estimate because some mineral thermometers have not equilibrated (*McSween and Patchen*, 1989).

The widely used temperature scale given by *Dodd* (1981) implies that peak temperatures increase from type 4 to 5 to 6. However, there is some evidence from mineral-equilibration thermometers that type 4 and 5 chondrites may have reached peak temperatures similar to those for type 6 chondrites, but then cooled more quickly (*Harvey et al.*, 1993; *Kessel et al.*, 2002). Additional work to separate peak temperature from cooling profile is clearly needed.

4.2. CO3 Chondrites

The least-metamorphosed CO3 chondrites, ALH A77307 (CO3.0) and Colony (CO3.0), probably experienced metamorphic temperatures of ~200°C, based on the absence of metamorphic effects on a micrometer scale in their silicates and on the abundances and characteristics of presolar grains (*Brearley*, 1993; *Huss et al.*, 2003; *Kobayashi et al.*, 2005). Kainsaz (CO3.2) may have been as hot as ~300°C (*Huss and Lewis*, 1994), similar to ordinary chondrites like Bishunpur (LL3.15). *Sears et al.* (1991a) argued on the basis of TL glow curves that the CO3 chondrites were heated to lower temperatures than type 3 ordinary chondrites, but for longer times. However, this conclusion is based in part on higher temperatures for type 3 ordinary chondrites (400°C for type 3.0–3.1 and 600°–700°C for type 3.6–3.8) than are currently favored (see above).

4.3. CV3 Chondrites

Assigning absolute temperatures to CV3 metamorphism is difficult because of their complex histories before and after accretion (see above). Precursor materials for matrix, the component where most temperature indicators are found, may have been heated significantly prior to accretion (*Huss et al.*, 2003). Despite these complications, *Huss and Lewis* (1994) used gas-release profiles from presolar diamonds and several methods of estimating temperature to infer maximum metamorphic temperatures of ~300°C for Leoville and Vigarano, two of the most primitive CV3$_{red}$ meteorites. Mokoia (CO3$_{ox}$ breccia) may have experienced a similar metamorphic temperature (*Huss et al.*, 2003). *Bonal et al.* (2004) placed the CV3 chondrites into a metamorphic sequence based on Raman spectroscopy of organic material and tied the resulting sequence to that for type 3 ordinary chondrites. Using the *Bonal et al.* (2004) sequence, the characteristics of presolar grains, and temperatures derived by *Huss and Lewis* (1994), the following approximate temperatures can be assigned to the CV3 chondrites: Leoville, ~250°C; Vigarano, Mokoia, Kaba, Efremovka, 300°–400°C; Grosnaja, ~500°C; Axtell, Allende, 550°–600°C.

4.4. Enstatite Chondrites

Enstatite chondrites in general seem to have experienced more-severe thermal and shock metamorphism than most other meteorites. *Huss and Lewis* (1994) used noble gases in presolar diamonds to estimate maximum temperatures for Qingzhen (EH3) and Indarch (EH4) of ~525°C and ~640°C, respectively. Disturbed ^{26}Al-^{26}Mg, ^{53}Mn-^{53}Cr, and ^{60}Fe-^{60}Ni systematics in E3 chondrules and sulfides (*Guan et al.*, 2004, 2005) also indicate that E3 chondrites experienced higher metamorphic temperatures than type 3.0–3.5 ordinary chondrites. Maximum metamorphic temperatures for E5 and E6 chondrites are poorly constrained. Various thermometers suggest that E6 chondrites reached temperatures similar to or somewhat higher than type 6 ordinary chondrites (*Dodd*, 1981). Equilibration temperatures for EH5 and EH6 chondrites were in the range of 800°–1000°C, but EL5 and EL6 chondrites may have equilibrated at 600°–800°C (*Zhang et al.*, 1996). Many enstatite chondrites exhibit evidence of

moderate to severe shock, which may have heated them to temperatures equal to or higher than their metamorphic temperatures after which they were rapidly quenched (*Rubin and Scott,* 1997). Separating effects of static and shock metamorphism is particularly difficult for enstatite chondrites.

4.5.   Other Classes

Temperatures of metamorphism for other chondrite classes are poorly determined. Renazzo (CR2) apparently was heated to ~150°–300°C on its parent body (*Huss et al.,* 2003, and references therein). CH and CB chondrites show little if any evidence of parent-body metamorphism (*Weisberg et al.,* 2001; *Krot et al.,* 2002), which implies similarly low temperatures. The metamorphic sequence shown by the CK chondrites suggests temperatures similar to those of ordinary chondrites (*Geiger and Bischoff,* 1991).

5.   OXIDATION STATE DURING METAMORPHISM

5.1.   Ordinary Chondrites

There is disagreement in the literature about the extent to which oxygen fugacity (f_{O_2}) may have changed as a function of metamorphic grade in ordinary chondrites. Observations relevant to this issue are (1) the amount of metal appears to increase from type 3 to 4 [e.g., ~11 vol% in H3 to ~16 vol% in H4–6 (*Lux et al.,* 1980)]; (2) the C abundance decreases from type 3 to 4 (Table 1); (3) the FeO content of olivine and pyroxene increases slightly but systematically from type 4 to 6 (*Scott et al.,* 1986; *Rubin,* 1990); (4) metal abundance decreases slightly from type 4 to 6 (*McSween and Labotka,* 1993); and (5) the Ni and Co content of metal increases slightly from type 4 to 6 (*Rubin,* 1990; *McSween and Labotka,* 1993).

Observations 1 and 2 imply that type 3 material was reduced by reactions with C as it was metamorphosed to type 4 (e.g., *Lux et al.,* 1980). However, the data are not as clear-cut as they first appear. Among H3 chondrite falls, Sharps has an anomalously low metal content (cf. *Jarosewich,* 1990) and is primarily responsible for the trend in H chondrites. Among L-chondrite falls, there is only a hint of a trend, and among LL falls, the type 3s seem to have higher metal contents than types 4–6 (*Jarosewich,* 1990). Thus, while reduction by C is reasonable, the data supporting the idea are not convincing.

Observations 3–5 have been interpreted to indicate oxidation during metamorphism from type 4–6 (*McSween and Labotka,* 1993). These authors also calculated oxygen fugacities from chondrite mineral equilibria and found that f_{O_2} increases slightly between types 4 and 6. Their results are at odds with earlier intrinsic f_{O_2} measurements, which appear to show reduction during metamorphism (*Brett and Sato,* 1984), and with earlier calculated oxygen fugacities (*McSween and Labotka,* 1993, and references therein). More recently, *Kessel et al.* (2004) found no evidence for

major shifts in f_{O_2} among type 4–6 H chondrites using olivine-orthopyroxene-metal assemblages, and they suggest that apparent changes in calculated f_{O_2} from type 4–6 might reflect higher peak temperatures for type 4 and 5 chondrites during metamorphism than are currently favored.

5.2.   Other Classes

Other chondrite classes were formed and metamorphosed under very different conditions. The R and CK chondrites are highly oxidized. They contain olivine that is enriched in FeO and NiO, they have low modal metal abundances, and the metal that is present tends to be Ni rich (*Rubin and Kallemeyn,* 1989; *Bischoff et al.,* 1994; *Geiger and Bischoff,* 1991). At the other extreme, enstatite chondrites are highly reduced and consist of FeO-free silicates and have high metal contents and a wide variety of exotic sulfides (e.g., *Dodd,* 1981). However, details of the metamorphic environments for these and other meteorite classes are not understood.

6.   HEAT SOURCES

Two fundamentally different scenarios have been proposed to explain the sequence of textural and compositional changes among chondritic meteorites. In the autometamorphism model (also known as "hot accretion"), batches of hot (~700°–900°C) material accreted to a parent body and began to cool (*Anders,* 1964; *Larimer and Anders,* 1967; *Hutchison et al.,* 1980; *Hutchison,* 1996). In this model, rapidly cooled material developed into type 3 chondrites, while very slowly cooled material became type 6 chondrites. *Rubin and Brearley* (1996) evaluated the arguments for hot accretion and concluded that this model is untenable. There is now a consensus that chondrites experienced prograde thermal metamorphism. In the prograde-metamorphism model, cold, unequilibrated material was progressively heated on a parent body (*Merrill,* 1921; *Wood,* 1962; *Van Schmus and Koffman,* 1967; *Dodd,* 1969; *Lux et al.,* 1980). The heat sources that have been proposed to drive prograde metamorphism in chondrites include energy from collisions, radioactive decay ([26]Al and [60]Fe), electromagnetic induction, and FU-Orionis-type events. The heat source(s) that metamorphosed chondrites may also have been responsible for melting some asteroids, producing differentiated meteorites (HEDs, mesosiderites, pallasites, angrites, and magmatic irons).

6.1.   Accretional or Collisional Heating

The accretion process that built asteroids from smaller planetesimals converted kinetic energy into heat. However, the amount of energy released during the gentle impacts that permitted asteroids to grow rather than disrupt is too small to have resulted in significant heating (*Wood and Pellas,* 1991). Once an asteroid formed, higher-velocity impacts could have deposited significant energy without disrupting

the body. There is a positive correlation between petrologic type and shock stage among ordinary chondrites (*Stöffler et al.,* 1991; *Rubin,* 1995, 2003), and there is also a correspondence among chondrite groups between those with many metamorphosed members and those with many shocked members (*Rubin,* 2004). Moreover, many type 5–6 ordinary chondrites of apparently low shock stage (S1) show evidence for annealing after an earlier episode of more intense shock (*Rubin,* 2004). These observations suggest that shock heating has played a significant role in metamorphism of ordinary chondrites.

6.2. Short-lived Radionuclides

Two short-lived radionuclides may have been significant heat sources: ^{26}Al and ^{60}Fe. Other radionuclides were also present, but either they were incorporated into parent bodies with abundances too low to produce significant heating (^{41}Ca, ^{10}Be), or because of long half-lives, heat generation was too slow to overcome heat loss (^{53}Mn).

6.2.1. Aluminum-26. The presence in the early solar system of live ^{26}Al ($t_{1/2} = 0.72$ m.y.) has been inferred from a wide variety of chondritic materials (e.g., *Lee et al.,* 1976; *MacPherson et al.,* 1995). The highest inferred initial ^{26}Al/^{27}Al ratios [$(^{26}$Al/^{27}Al$)_0$] are from CAIs, and the canonical initial ratio for the solar system ($\sim 5 \times 10^{-5}$) has been derived from CAI data. Advocates of ^{26}Al heating generally assume that this isotope was homogeneously distributed in the solar system. Chondrules in ordinary chondrites have lower inferred $(^{26}$Al/^{27}Al$)_0$ ratios ($\sim 1 \times 10^{-5}$), indicating that they formed ~ 2 m.y. after CAIs (*Kita et al.,* 2000, 2005). Accretion of chondritic asteroids probably postdated chondrule formation. Asteroid thermal evolution models based on these assumptions show that an asteroid of ~ 100 km in diameter could have reached a maximum temperature of $>1000°C$ at its center and sustained it for more than 10 m.y. (*Miyamoto et al.,* 1981; *Bennett and McSween,* 1996; *McSween et al.,* 2002). This is ample heating to account for metamorphism in ordinary chondrites.

6.2.2. Iron-60. Recent work has shown that ^{60}Fe ($t_{1/2} = 1.5$ m.y.) was incorporated into chondritic meteorites with inferred $(^{60}$Fe/^{56}Fe$)_0$ ratios of between $\sim 3 \times 10^{-7}$ and $\sim 1 \times 10^{-6}$ (*Tachibana and Huss,* 2003; *Tachibana et al.,* 2005; *Mostefaoui et al.,* 2003). If incorporated into chondrites at this level, ^{60}Fe would have been able to raise the internal temperatures of asteroids with LL and CV compositions by 140°C and 170°C, respectively (*Kunihiro et al.,* 2004). Thus, ^{60}Fe would have been a significant secondary heat source for metamorphism.

6.3. Electromagnetic Induction

The active pre-main-sequence Sun emitted an intense, high-density, at least partly ionized solar wind at an outflow velocity of several hundred kilometers per second. Such a wind would have carried an embedded magnetic field and might have been capable of driving electrical currents in asteroids that were sufficiently conductive (e.g., *Herbert and Sonett,* 1979; *Herbert,* 1989). Heating would have occurred in the asteroid interior where heat is more efficiently retained. However, T Tauri stars blow off much of their mass at their poles, not at the midplane where asteroids would reside, and induction-heating models typically assume unrealistically high outflow velocities and solar wind fluxes (*Wood and Pellas,* 1991). Most workers do not currently believe that electromagnetic induction was a significant source of asteroidal heating.

6.4. FU-Orionis-type Events

Pre-main-sequence stars apparently experience periodic outbursts during which brightness increases dramatically (up to a factor of 250) over periods as short as 1 year and then decreases to pre-outburst levels over 10–100 years (*Herbig,* 1978; *Bell et al.,* 2000). T Tauri stars may be in an outburst state $\sim 10\%$ of the time. *Wasson* (1992) suggested that these outbursts could have heated the outer ~ 100 m of planetesimals at a distance of ~ 3 AU to $>1200°C$ for several hundred years. This type of heating would occur only if the nebula had largely cleared between the Sun and the asteroids. However, the outbursts primarily occur when stars have massive accretion disks (*Bell et al.,* 2000). As a consequence, most workers do not consider this heating mechanism to be viable.

7. TIMESCALE FOR METAMORPHISM

Estimates of metamorphic timescales come primarily from radiometric age dating, supported in some cases by estimates of cooling rates. Essentially all applicable data come from ordinary chondrites. Short-lived nuclides provide constraints on the early stages of the metamorphic epoch, if these nuclides were distributed homogeneously in the early solar system. The inferred $(^{26}$Al/^{27}Al$)_0$ ratios for chondrules from Semarkona (LL3.00) and Bishunpur (LL3.15) indicate that chondrule formation took place 1–2 m.y. after CAIs (*Kita et al.,* 2000, 2005). Inferred $(^{60}$Fe/^{56}Fe$)_0$ ratios for chondrules, magnetite, and sulfides in Semarkona, Bishunpur, and Krymka (LL3.2) imply that parent-body alteration of these meteorites took place 0.5–2.0 m.y. after chondrules formed (*Tachibana et al.,* 2005). The $(^{26}$Al/^{27}Al$)_0$ ratios for a glassy clast from Bovedy (L3.7) and for plagioclase from Ste. Marguerite (H4) imply that these meteorites had cooled below the blocking temperature for the Al-Mg system by ~ 6 m.y. after CAIs formed, and the upper limit on $(^{26}$Al/^{27}Al$)_0$ for a basaltic clast from Barwell (L6) implies that Barwell did not cool down until at least 7 m.y. after CAIs formed (*Huss et al.,* 2001). These data imply that, relative to the time of CAI formation, accretion of ordinary chondrites took place ~ 2 m.y. later, metamorphism of type 3.0–3.2 chondrites took place between 2 and 4 m.y. later, in type 3.7–4 chondrites lasted until ~ 6 m.y. later, and in type 6 chondrites continued for >7 m.y. after CAIs formed.

Data for [244]Pu-fission-track and Pb-Pb dating give a coherent picture of H-chondrite metamorphism and appear to support an onion-shell model for the H-chondrite parent body (*Trieloff et al.,* 2003). The two methods have different closure temperatures and thus date different points in the cooling history of the H-chondrite parent body. The Pb-Pb ages, which reflect cooling below ~750 K, indicate that metamorphism of H4 chondrites was ending 4–6 m.y. after CAIs, consistent with estimates from [26]Al. Lead-lead data further suggest that metamorphism ended for H5 and H6 chondrites 10–16 m.y. and 45–63 m.y. after CAIs, respectively. Fission tracks are retained at ~550 K (pyroxene) or ~390 K (merrilite), so [244]Pu fission track ages reflect a later stage in the cooling history. These ages indicate that metamorphism ended ~10 m.y. for H4, 50–65 m.y. for H5, and 55–65 m.y. for H6 chondrites after CAIs formed (*Trieloff et al.,* 2003). These cooling times are generally consistent with [26]Al (and [60]Fe) as the heat source for metamorphism (cf. *Ghosh and McSween,* 1998). However, an extensive set of metallographic cooling rates for H chondrites, many of which were not studied by *Trieloff et al.* (2003), do not show a consistent relationship between cooling rate and petrologic type (*Taylor et al.,* 1987), suggesting that the H-chondrite parent body did not have an onion-shell structure, or if it did, that this structure was disrupted before the parent body cooled below ~800 K.

REFERENCES

Afiattalab F. and Wasson J. T. (1980) Composition of the metal phases in ordinary chondrites: Implications regarding classification and metamorphism. *Geochim. Cosmochim. Acta, 44,* 431–446.

Alaerts L., Lewis R. S., and Anders E. (1979) Isotopic anomalies of noble gases in meteorites and their origins — III. LL-chondrites. *Geochim. Cosmochim. Acta, 43,* 1399–1425.

Alexander C. M. O'D., Barber D. J., and Hutchison R. H. (1989a) The microstructure of Semarkona and Bishunpur. *Geochim. Cosmochim. Acta, 53,* 3045–3057.

Alexander C. M. O'D., Hutchison R., and Barber D. J. (1989b) Origin of chondrule rims and interchondrule matrices in unequilibrated ordinary chondrites. *Earth Planet. Sci. Lett., 95,* 187–207.

Alexander C. M. O'D., Grossman J. N., Wang J., Zanda B., Bourot-Denise M., and Hewins R. H. (2000) The lack of potassium-isotopic fractionation in Bishunpur chondrules. *Meteoritics & Planet. Sci., 35,* 859–868.

Anders E. (1964) Origin, age and composition of meteorites. *Space Sci. Rev., 3,* 583–714.

Ashworth J. R. (1977) Matrix textures in unequilibrated ordinary chondrites. *Earth Planet. Sci. Lett., 35,* 25–34.

Ashworth J. R. and Barber D. J. (1976) Lithification of gas-rich meteorites. *Earth Planet. Sci. Lett., 30,* 222–223.

Bell K. R., Cassen P. M., Wasson J. T., and Woolum D. S. (2000) The FU Orionis phenomenon and solar nebula material. In *Protostars and Planets IV* (V. Mannings et al., eds.), pp. 897–926. Univ. of Arizona, Tucson.

Bennett M. E. III and McSween H. Y. Jr. (1996) Revised model calculations for the thermal histories of ordinary chondrite parent bodies. *Meteoritics, 31,* 783–792.

Benoit P. H., Akridge G., and Sears D. W. G. (1998) Size sorting of metal, sulfide, and chondrules in Sharps (H3.4) (abstract). In *Lunar and Planetary Science XXIX,* Abstract #1457. Lunar and Planetary Institute, Houston (CD-ROM).

Benoit P. H., Akridge G. A., Ninagawa K., and Sears D. W. G. (2002) Thermoluminescence sensitivity and thermal history of type 3 ordinary chondrites: Eleven new type 3.0–3.1 chondrites and possible explanations for differences among H, L, and LL chondrites. *Meteoritics & Planet. Sci., 37,* 793–805.

Bischoff A. (2000) Mineralogical characterization of primitive, type-3 lithologies in Rumuruti chondrites. *Meteoritics & Planet. Sci., 35,* 699–706.

Bischoff A., Geiger T., Palme H., Spettel B., Schultz L., Scherer P., Loeken T., Bland P., Clayton R. N., Mayeda T. K., Herpers U., Meltzow B., Michel R. and Dittrich-Hannen B. (1994) Acfer 217 — A new member of the Rumuruti chondrite group (R). *Meteoritics, 29,* 264–274.

Binns R. A. (1967) Olivine in enstatite chondrites. *Am. Mineral., 52,* 1549–1554.

Bonal L., Quirico E., and Bourot-Denise M. (2004) Petrologic type of CV3 chondrites as revealed by Raman spectroscopy of organic matter (abstract). In *Lunar and Planetary Science XXXV,* Abstract #1562. Lunar and Planetary Institute, Houston (CD-ROM).

Boyd F. R. and England J. L. (1965) The rhombic enstatite-clinoenstatite inversion. In *Year Book — Carnegie Institution of Washington,* pp. 117–120. Carnegie Institution of Washington, Washington, DC.

Brearley A. J. (1990) Carbon-rich aggregates in type 3 ordinary chondrites: Characterization, origins, and thermal history. *Geochim. Cosmochim. Acta, 54,* 831–850.

Brearley A. J. (1993) Matrix and fine-grained rims in the unequilibrated CO3 chondrite, ALHA77307: Origins and evidence for diverse, primitive nebular dust components. *Geochim. Cosmochim. Acta, 57,* 1521–1550.

Brearley A. J. (1995) Nature of matrix in unequilibrated chondrites and its possible relationship to chondrules. In *Chondrules and the Protoplanetary Disk* (R. H. Hewins et al., eds.), pp. 137–151. Cambridge Univ., Cambridge.

Brearley A. J. and Jones R. H. (1998) Chondritic meteorites. In *Planetary Materials* (J. J. Papike, ed.,) pp. 3-1 to 3-398. Reviews in Mineralogy, Vol. 36, Mineralogical Society of America.

Brett R. and Sato M. (1984) Intrinsic oxygen fugacity measurements on seven chondrites, a pallasite, and a tektite and the redox state of meteorite parent bodies. *Geochim. Cosmochim. Acta, 48,* 111–120.

Chizmadia L. J. (2000) Amoeboid olivine inclusions in CO3 carbonaceous chondrites: Sensitive indicators of parent body aqueous alteration. Master's thesis, Univ. of California, Los Angeles.

Chizmadia L. J., Rubin A. E., and Wasson J. T. (2002) Mineralogy and petrology of amoeboid olivine inclusions in CO3 chondrites: Relationship to parent-body aqueous alteration. *Meteoritics & Planet. Sci., 38,* 1781–1796.

Christophe Michel-Levy M. (1976) La matrice noire et blanche de la chondrite de Tieschitz (H3). *Earth Planet. Sci. Lett., 30,* 143–150.

Crabb J. and Anders E. (1981) Noble gases in E-chondrites. *Geochim. Cosmochim. Acta, 45,* 2443–2464.

Crabb J. and Anders E. (1982) On the siting of noble gases in E-chondrites. *Geochim. Cosmochim. Acta, 46,* 2351–2361.

DeHart J. M., Lofgren G. E., Lu J., Benoit P. H., and Sears D. W. G. (1992) Chemical and physical studies of chondrules X. Cathodoluminescence and phase composition studies of metamorphism and nebular processes in chondrules of type 3 ordinary chondrites. *Geochim. Cosmochim. Acta, 56,* 3791–3807.

Dodd R. T. (1969) Metamorphism of the ordinary chondrites: A review. *Geochim. Cosmochim. Acta, 33,* 161–203.

Dodd R. T. (1981) *Meteorites — A Petrologic-Chemical Synthesis.* Cambridge, New York. 368 pp.

Dodd R. T., Van Schmus W. R., and Koffman D. M. (1967) A survey of the unequilibrated ordinary chondrites. *Geochim. Cosmochim. Acta, 31,* 921–951.

Dodd R. T., Grover J. E., and Brown G. E. (1975) Pyroxenes in the Shaw (L-7) chondrite. *Geochim. Cosmochim. Acta, 39,* 1585–1594.

Geiger T. and Bischoff A. (1991) The CK chondrites — Conditions of parent body metamorphism. *Meteoritics, 26,* 337.

Ghosh A. and McSween H. Y. Jr. (1998) A thermal model for the differentiation of asteroid 4 Vesta based on radiogenic heating. *Icarus, 134,* 187–206.

Grossman J. N. and Brearley A. J. (2005) The onset of metamorphism in ordinary and carbonaceous chondrites. *Meteoritics & Planet. Sci., 40,* 87–122.

Grossman J. N., Zolensky M. E., and Tonui E. K. (2005) What are the petrologic types of thermally metamorphosed CM chondrites? (abstract). *Meteoritics & Planet. Sci., 40,* A61.

Guan Y., Huss G. R., and Leshin L. A. (2004) Further observations of ^{60}Fe-^{60}Ni and ^{53}Mn-^{53}Cr systems in sulfides from enstatite chondrites (abstract). In *Lunar and Planetary Science XXXV,* Abstract #2003. Lunar and Planetary Institute, Houston (CD-ROM).

Guan Y., Huss G. R., Leshin L. A., MacPherson G. J., and McKeegan K. D. (2005) Oxygen isotopes and ^{26}Al/^{26}Mg systematics of aluminum-rich chondrules from unequilibrated enstatite chondrites. *Meteoritics & Planet. Sci., 40,* in press.

Guimon R. K., Keck D. B., Weeks S. K., Dehart J., and Sears G. (1985) Chemical and physical studies of type 3 chondrites — IV: Annealing studies of a type 3, 4 ordinary chondrite and the metamorphic history of meteorites. *Geochim. Cosmochim. Acta, 49,* 1515–1524.

Guimon R. K., Lofgren G. E., and Sears D. W. G. (1988) Chemical and physical studies of type 3 chondrites. IX: Thermoluminescence and hydrothermal annealing experiments and their relationship to metamorphism and aqueous alteration in type <3.3 ordinary chondrites. *Geochim. Cosmochim. Acta, 52,* 119–127.

Guimon R. K., Symes S. J. K., Sears D. W. G., and Benoit P. H. (1995) Chemical and physical studies of type 3 chondrites XII: The metamorphic history of CV chondrites and their components. *Meteoritics, 30,* 704–714.

Harvey R. P., Bennett M. L., and McSween H. Y. Jr. (1993) Pyroxene equilibration temperatures in metamorphosed ordinary chondrites (abstract). In *Lunar and Planetary Science XXIV,* pp. 615–616. Lunar and Planetary Institute, Houston.

Herbert F. (1989) Primordial electrical induction heating of asteroids. *Icarus, 78,* 402–410.

Herbert F. and Sonett C. P. (1979) Electromagnetic heating of minor planets in the early solar system. *Icarus, 40,* 484–496.

Herbig G. H. (1978) Some aspects of early stellar evolution that may be relevant to the origin of the solar system. In *The Origin of the Solar System* (S. F. Dermott, ed.), pp. 219–235. Wiley, New York.

Housley R. M. and Cirlin E. H. (1983) On the alteration of Allende chondrules and the formation of matrix. In *Chondrules and Their Origins* (E. A. King, ed.), pp. 145–161. Lunar and Planetary Institute, Houston.

Hua X., Huss G. R., Tachibana S., and Sharp T. G. (2005) Oxygen, silicon, and Mn-Cr isotopes of fayalite in the Kaba oxidized CV3 chondrite: Constraints for its formation history. *Geochim. Cosmochim. Acta, 69,* 1333–1348.

Huss G. R. (1979) The matrix of unequilibrated ordinary chondrites: Implications for the origin and subsequent history of chondrites. Master's thesis, Univ. of New Mexico, Albuquerque.

Huss G. R. (1990) Ubiquitous interstellar diamond and SiC in primitive chondrites: Abundances reflect metamorphism. *Nature, 347,* 159–162.

Huss G. R. and Lewis R. S. (1994) Noble gases in presolar diamonds II: Component abundances reflect thermal processing. *Meteoritics, 29,* 811–829.

Huss G. R. and Lewis R. S. (1995) Presolar diamond, SiC, and graphite in primitive chondrites: Abundances as a function of meteorite class and petrologic type. *Geochim. Cosmochim. Acta, 59,* 115–160.

Huss G. R., Keil K., and Taylor G. J. (1978) Composition and recrystallization of the matrix of unequilibrated (type 3) ordinary chondrites (abstract). *Meteoritics, 13,* 495.

Huss G. R., Keil K., and Taylor G. J. (1981) The matrices of unequilibrated ordinary chondrites: Implications for the origin and history of chondrites. *Geochim. Cosmochim. Acta, 45,* 33–51.

Huss G. R., Lewis R. S., and Hemkin S. (1996) The "normal planetary" noble gas component in primitive chondrites: Compositions, carrier, and metamorphic history. *Geochim. Cosmochim. Acta, 60,* 3311–3340.

Huss G. R., MacPherson G. J., Wasserburg G. J., Russell S. S., and Srinivasan G. (2001) Aluminum-26 in calcium-aluminum-rich inclusions and chondrules from unequilibrated ordinary chondrites. *Meteoritics & Planet. Sci., 36,* 975–997.

Huss G. R., Meshik A. P., Smith J. B., and Hohenberg C. M. (2003) Presolar diamond, silicon carbide, and graphite in carbonaceous chondrites: Implications for thermal processing in the solar nebula. *Geochim. Cosmochim. Acta, 67,* 4823–4848.

Hutchison R. (1996) Hot accretion of the ordinary chondrites: The rocks don't lie (abstract). In *Lunar and Planetary Science XXVII,* pp. 579–580. Lunar and Planetary Institute, Houston.

Hutchison R., Bevan A. W. R., Agrell S. O., and Ashworth J. R. (1980) Thermal history of the H-group of chondritic meteorites. *Nature, 287,* 787–790.

Hutchison R., Alexander C. M. O'D., and Barber D. J. (1987) The Semarkona meteorite; first recorded occurrence of smectite in an ordinary chondrite, and its implication. *Geochim. Cosmochim. Acta, 51,* 1875–1882.

Itoh D. and Tomeoka K. (2003) Dark inclusions in CO3 chondrites: New indicators of parent-body processes. *Geochim. Cosmochim. Acta, 67,* 153–169.

Jarosewich E. (1990) Chemical-analyses of meteorites — A compilation of stony and iron meteorite analyses. *Meteoritics, 25,* 323–337.

Jones R. H. and Lofgren G. E. (1993) A comparison of FeO-rich, porphyritic olivine chondrules in unequilibrated chondrites and experimental analogues. *Meteoritics, 28,* 213–221.

Kallemeyn G. W. and Rubin A. E. (1995) Coolidge and Loongana-001 — A new carbonaceous chondrite grouplet. *Meteoritics, 30,* 20–27.

Kallemeyn G. W., Rubin A. E., Wang D., and Wasson J. T. (1989) Ordinary chondrites: Bulk compositions, classification, lithophile-element fractionations, and composition-petrographic type relationships. *Geochim. Cosmochim. Acta, 53,* 2747–2767.

Kallemeyn G. W., Rubin A. E., and Wasson J. T. (1991) The compositional classification of chondrites: V. The Karoonda (CK) group of carbonaceous chondrites. *Geochim. Cosmochim. Acta, 55,* 881–892.

Kallemeyn G. W., Rubin A. E., and Wasson J. T. (1996) The compositional classification of chondrites: VII. The R chondrite group. *Geochim. Cosmochim. Acta, 60,* 2243–2256.

Keller L. P. and Buseck P. R. (1990) Matrix mineralogy of the Lancé CO3 carbonaceous chondrite: A transmission electron microscope study. *Geochim. Cosmochim. Acta, 54,* 1155–1163.

Kessel R., Beckett J. R., and Stolper E. M. (2002) The thermal history of equilibrated ordinary chondrites and the relationship between textural maturity and temperature (abstract). In *Lunar and Planetary Science XXXIII,* Abstract #1420. Lunar and Planetary Institute, Houston (CD-ROM).

Kessel R., Beckett J. R., Huss G. R., and Stolper E. M. (2004) The activity of chromite in multicomponent spinels: Implications for T-f_{O_2} conditions of equilibrated H chondrites. *Meteoritics & Planet. Sci., 39,* 1287–1305.

Kimura M. and Ikeda Y. (1995) Anyhdrous alteration of Allende chondrules in the solar nebula. II: Alkali-Ca exchange reactions and formation of nepheline, sodalite and Ca-rich phases in chondrules. *Proc. NIPR Symp. Antarct. Meteorites, 8,* 123–138.

Kita N. T., Nagahara H., Togashi S., and Morishita Y. (2000) A short duration of chondrule formation in the solar nebula: Evidence from [26]Al in Semarkona ferromagnesian chondrules. *Geochim. Cosmochim. Acta, 64,* 3913–3922.

Kita N. T., Huss G. R., Tachibana S., Amelin Y., Nyquist L. E., and Hutcheon I. D. (2005) Constraints on the origin of chondrules and CAIs from short-lived radionuclides. In *Chondrites and the Protoplanetary Disk* (A. N. Krot et al., eds.), pp. 558–587. ASP Conference Series 341, Astronomical Society of the Pacific, San Francisco.

Kobayashi S., Tonotani A., Sakamoto K., Nagashima K, Krot A. N., and Yurimoto H. (2005) Presolar silicate grains from primitive carbonaceous chondrites Y-81025, ALHA 77307, Adelaide and Acfer 094 (abstract). In *Lunar and Planetary Science XXXVI,* Abstract #1931. Lunar and Planetary Institute, Houston (CD-ROM).

Krot A. N., Scott E. R. D., and Zolensky M. E. (1995) Mineralogical and chemical modification of components in CV3 chondrites: Nebular or asteroidal processing? *Meteoritics, 30,* 748–775.

Krot A. N., Zolensky M. E., Wasson J. T., Scott E. R. D., Keil K., and Oshumi K. (1997) Carbide-magnetite assemblages in type 3 ordinary chondrites. *Geochim. Cosmochim. Acta, 61,* 219–237.

Krot A. N., Petaev M. I., Scott E. R. D., Choi B.-G., Zolensky M. E., and Keil K. (1998a) Progressive alteration in CV3 chondrites: More evidence for asteroidal alteration. *Meteoritics & Planet. Sci., 33,* 1065–1085.

Krot A. N., Petaev M. I., Zolensky M. E., Keil K., Scott E. R. D., and Nakamura K. (1998b) Secondary calcium-iron-rich minerals in the Bali-like and Allende-like oxidized CV3 chondrites and Allende dark inclusions. *Meteoritics & Planet. Sci., 33,* 623–645.

Krot A. N., Meibom A., Weisberg M. K., and Keil K. (2002) The CR chondrite clan: Implications for early solar system processes. *Meteoritics & Planet. Sci., 37,* 1451–1490.

Kunihiro T., Rubin A. E., McKeegan K. D., and Wasson J. T. (2004) Initial [26]Al/[27]Al in carbonaceous-chondrite chondrules: Too little [26]Al to melt asteroids. *Geochim. Cosmochim. Acta, 68,* 2947–2957.

Larimer J. W. and Anders E. (1967) Chemical fractionation of meteorites, II. Abundance patterns and their interpretation. *Geochim. Cosmochim. Acta, 31,* 1239–1270.

Lee T., Papanastassiou D. A., and Wasserburg G. J. (1976) Demonstration of Mg-26 excess in Allende and evidence for Al-26. *Geophys. Res. Lett., 3,* 41–44.

Lipschutz M. E. and Woolum D. S. (1988) Highly labile elements. In *Meteorites and the Early Solar System* (J. F. Kerridge and M. S. Matthews, eds.), pp. 462–487. Univ. of Arizona, Tucson.

Lux G., Keil K. and Taylor G. J. (1980) Metamorphism of the H-group chondrites: Implications from compositional and textural trends in chondrules. *Geochim. Cosmochim. Acta, 44,* 841–855.

MacPherson G. J., Davis A. M., and Zinner E. K. (1995) The distribution of aluminum-26 in the early solar system — A reappraisal. *Meteoritics, 30,* 365–386.

McCoy T. J., Scott E. R. D., Jones R. H., Keil K., and Taylor G. J. (1991) Composition of chondrule silicates in LL3–5 chondrites and implications for their nebular history and parent body metamorphism. *Geochim. Cosmochim. Acta, 55,* 601–619.

McCoy T. J., Keil K., Bogard D. D., Garrison D. H., Casanova I., Lindstrom M. M., Brearley A. J., Kehm K., Nichols R. H. Jr., and Hohenberg C. M. (1995) Origin and history of impact-melt rocks of enstatite chondrite parentage. *Geochim. Cosmochim. Acta, 59,* 161–175.

McSween H. Y. Jr. (1977a) Carbonaceous chondrites of the Ornans type: A metamorphic sequence. *Geochim. Cosmochim. Acta, 41,* 477–491.

McSween H. Y. Jr. (1977b) Petrographic variations among carbonaceous chondrites of the Vigarano type. *Geochim. Cosmochim. Acta, 41,* 1777–1790.

McSween H. Y. Jr. (1979) Are carbonaceous chondrites primitive or processed? A review. *Rev. Geophys. Space Phys., 17,* 1059–1078.

McSween H. Y. Jr. and Labotka T. C. (1993) Oxidation during metamorphism of the ordinary chondrites. *Geochim. Cosmochim. Acta, 57,* 1105–1114.

McSween H. Y. Jr. and Patchen A. D. (1989) Pyroxene thermobarometry in LL-group chondrites and implications for parent body metamorphism. *Meteoritics, 24,* 219–226.

McSween H. Y. Jr., Ghosh A., Grimm R. E., Wilson L., and Young E. D. (2002) Thermal evolution models of asteroids. In *Asteroids III* (W. F. Bottke Jr. et al., eds.), pp. 559–571. Univ. of Arizona, Tucson.

Merrill G. P. (1921) On metamorphism in meteorites. *Geol. Soc. Am. Bull., 32,* 395–416.

Methot R. L., Noonan A. F., Jarosewich E., Al-Far D. M., and Degasparis A. A. (1975) Mineralogy, petrology and chemistry of the Isna C3 meteorite. *Meteoritics, 10,* 121–130.

Mittlefehldt D. W. and Lindstrom M. M. (2001) Petrology and geochemistry of Patuxent Range 91501, a clast-poor impact melt from the L-chondrite parent body and Lewis Cliff 88663, an L7 chondrite. *Meteoritics & Planet. Sci., 36,* 439–457.

Miyamoto M., Fujii N., and Takeda H. (1981) Ordinary chondrite parent body: An internal heating model. *Proc. Lunar Planet. Sci. 12B,* pp. 1145–1152.

Mostefaoui S., Lugmair G. W., Hoppe P., and El Goresy A. (2003) Evidence for live iron-60 in Semarkona and Chervony Kut: A nanoSIMS study (abstract). In *Lunar and Planetary Science XXXIV,* Abstract #1585. Lunar and Planetary Institute, Houston (CD-ROM).

Mostefaoui S., Marhas K. K., and Hoppe P. (2004) Discovery of an in-situ presolar silicate grain with GEMS-like composition in the Bishunpur matrix (abstract). In *Lunar and Planetary Science XXXV,* Abstract #1593. Lunar and Planetary Institute, Houston (CD-ROM).

Nagahara H. (1984) Matrices of type 3 ordinary chondrites — primitive nebular records. *Geochim. Cosmochim. Acta, 48,* 2581–2595.

Nittler L. R. (2003) Presolar stardust in meteorites: Recent advances and scientific frontiers. *Earth Planet. Sci. Lett., 209,* 259–273.

Olsen E. J. and Bunch T. E. (1984) Equilibration temperatures of the ordinary chondrites: A new evaluation. *Geochim. Cosmochim. Acta, 48,* 1363–1365.

Olsen E., Bunch T., Jarosewich E., and Huss G. I. (1976) Happy Canyon: An E7 enstatite chondrite. *Meteoritics, 11,* 348–349.

Palme H. and Wark D. A. (1988) CV-chondrites: High temperature gas-solid equilibrium vs. parent body metamorphism (abstract). In *Lunar and Planetary Science XIX,* p. 897. Lunar and Planetary Institute, Houston.

Peck J. A. and Wood J. A. (1987) The origin of ferrous zoning in Allende chondrule olivine. *Geochim. Cosmochim. Acta, 51,* 1503–1510.

Prinz M., Nehru C. E., Weisberg M. K., and Delaney J. S. (1984) Type 3 enstatite chondrites: A newly recognized group of unequilibrated enstatite chondrites (UEC's) (abstract). In *Lunar and Planetary Science XIV,* pp. 653–654. Lunar and Planetary Institute, Houston.

Rambaldi E. R. and Wasson J. T. (1981) Metal and associated phases in Bishunpur, a highly unequilibrated ordinary chondrite. *Geochim. Cosmochim. Acta, 45,* 1001–1015.

Reed S. J. B. (1968) Perryite in the Kota-Kota and South Oman enstatite chondrites. *Mineral. Mag., 36,* 850–854.

Reitmeijer F. J. M. and MacKinnon I. D. R. (1985) Poorly graphitized carbon as a new cosmothermometer for primitive extraterrestrial materials. *Nature, 315,* 733–736.

Rubin A. E. (1984) Coarse-grained chondrule rims in type 3 chondrites. *Geochim. Cosmochim. Acta, 48,* 1779–1789.

Rubin A. E. (1990) Kamacite and olivine in ordinary chondrites: Intergroup and intragroup relationships. *Geochim. Cosmochim. Acta, 54,* 1217–1232.

Rubin A. E. (1995) Petrologic evidence for collisional heating of chondritic asteroids. *Icarus, 113,* 156–167.

Rubin A. E. (1998) Correlated petrologic and geochemical characteristics of CO3 chondrites. *Meteoritics & Planet. Sci., 33,* 385–391.

Rubin A. E. (2000) Petrologic, geochemical and experimental constraints on models of chondrule formation. *Earth Sci. Rev., 50,* 3–27.

Rubin A. E. (2003) Chromite-plagioclase assemblages as a new shock indicator; implications for the shock and thermal histo-ries of ordinary chondrites. *Geochim. Cosmochim. Acta, 67,* 2695–2709.

Rubin A. E. (2004) Post-shock annealing and post-annealing shock in equilibrated ordinary chondrites: Implications for the thermal and shock histories of chondritic asteroids. *Geochim. Cosmochim. Acta, 68,* 673–689.

Rubin A. E. and Brearley A. J. (1996) A critical evaluation of the evidence for hot accretion. *Icarus, 124,* 86–96.

Rubin A. E. and Grossman J. N. (1985) Phosphate-sulfide assemblages and Al/Ca ratios in type-3 chondrites. *Meteoritics, 20,* 479–489.

Rubin A. E. and Kallemeyn G. W. (1989) Carlisle Lakes and Allan Hills 85151: Members of a new chondrite grouplet. *Geochim. Cosmochim. Acta, 53,* 3035–3044.

Rubin A. E. and Scott E. R. D. (1997) Abee and related EH chondrite impact-melt breccias. *Geochim. Cosmochim. Acta, 61,* 425–435.

Rubin A. E., Scott E. R. D., and Keil K. (1997) Shock metamorphism of enstatite chondrites. *Geochim. Cosmochim. Acta, 61,* 847–858.

Rubin A. E., Ulff-Møller F., Wasson J. T., and Carlson W. D. (2001) The Portales Valley meteorite breccia: Evidence for impact-induced melting and metamorphism of an ordinary chondrite. *Geochim. Cosmochim. Acta, 65,* 323–342.

Russell S. S., Huss G. R., Fahey A. J., Greenwood R. C., Hutchison R. and Wasserburg G. J. (1998) An isotopic and petrologic study of calcium-aluminum-rich inclusions from CO3 meteorites. *Geochim. Cosmochim. Acta, 62,* 689–714.

Russell S. S., MacPherson G. J., Leshin L. A., and McKeegan K. D. (2000) ^{16}O enrichments in aluminum-rich chondrules from ordinary chondrites. *Earth Planet. Sci. Lett., 184,* 57–74.

Scott E. R. D. and Jones R. H. (1990) Disentangling nebular and asteroidal features of CO3 carbonaceous chondrite meteorites. *Geochim. Cosmochim. Acta, 54,* 2485–2502.

Scott E. R. D. and Krot A. N. (2003) Chondrites and their components. In *Treatise on Geochemistry, Vol. 1: Meteorites, Comets, and Planets* (A. M. Davis, ed.), pp. 143–200. Elsevier, Oxford.

Scott E. R. D., Taylor G. J., and Keil K. (1986) Accretion, metamorphism, and brecciation of ordinary chondrites: Evidence from petrologic studies of meteorites from Roosevelt County, New Mexico. *Proc. Lunar Planet. Sci. Conf. 17th,* in *J. Geophys. Res., 91,* E115–E123.

Scott E. R. D., Barber D. J., Alexander C. M. O'D., Hutchison R., and Peck J. A. (1988) Primitive material surviving in chondrites; matrix. In *Meteorites and the Early Solar System* (J. F. Kerridge and M. S. Matthews, eds.), pp. 718–745. Univ. of Arizona, Tucson.

Scott E. R. D., Keil K., and Stöffler D. (1992) Shock metamorphism of carbonaceous chondrites. *Geochim. Cosmochim. Acta, 56,* 4281–4293.

Scott E. R. D., Jones R. H., and Rubin A. E. (1994) Classification, metamorphic history, and pre-metamorphic composition of chondrules. *Geochim. Cosmochim. Acta, 58,* 1203–1209.

Sears D. W. G., Grossman J. N., Melcher C. L., Ross L. M., and Mills A. A. (1980) Measuring metamorphic history of unequilibrated ordinary chondrites. *Nature, 287,* 791–795.

Sears D. W. G., Grossman J. N., and Melcher C. L. (1982a) Chemical and physical studies of type 3 chondrites — I: Metamorphism related studies of Antarctic and other type 3 ordinary chondrites. *Geochim. Cosmochim. Acta, 46,* 2471–2481.

Sears D. W., Kallemeyn G. W., and Wasson J. T. (1982b) The compositional classification of chondrites: II. The enstatite

chondrite groups. *Geochim. Cosmochim. Acta, 46,* 597–608.

Sears D. W. G., DeHart J. M., Hasan F. A., and Lofgren G. E. (1990) Induced thermoluminescence and cathodoluminescence studies of meteorites. In *Spectroscopic Characterization of Minerals and Their Surfaces* (L. M. Coyné et al., eds.), pp. 190–222. American Chemical Society, Washington, DC.

Sears D. W. G., Batchelor J. D., Lu J., and Keck B. D. (1991a) Metamorphism of CO and CO-like chondrites and comparisons with type 3 ordinary chondrites. *Proc. NIPR Symp. Antarct. Meteorites, 4,* 319–343.

Sears D. W. G., Hasan E. A., Batchelor J. D., and Lu J. (1991b) Chemical and physical studies of type 3 chondrites — XI: Metamorphism, pairing, and brecciation of ordinary chondrites. *Proc. Lunar Planet. Sci. Conf., Vol. 21,* pp. 493–512.

Sears D. W. G., Huang S., and Benoit P. H. (1995) Chondrule formation, metamorphism, brecciation, an important new primary chondrule group, and the classification of chondrules. *Earth Planet. Sci. Lett., 131,* 27–39.

Srinivasan G., Huss G. R., and Wasserburg G. J. (2000) A petrographic, chemical, and isotopic study of calcium-aluminum-rich inclusions and aluminum-rich chondrules from the Axtell (CV3) chondrite. *Geochim. Cosmochim. Acta, 35,* 1333–1354.

Stöffler D., Keil K., and Scott E. E R D. (1991) Shock metamorphism of ordinary chondrites. *Geochim. Cosmochim. Acta, 55,* 3845–3867.

Tachibana S. and Huss G. R. (2003) The initial abundance of ^{60}Fe in the solar system. *Astrophys. J. Lett., 588,* L41–L44.

Tachibana S., Huss G. R., Kita N. T., Shimoda H., and Morishita Y. (2005) The abundances of iron-60 in pyroxene chondrules from unequilibrated ordinary chondrites (abstract). In *Lunar and Planetary Science XXXVI,* Abstract #1529. Lunar and Planetary Institute, Houston (CD-ROM).

Tandon S. N. and Wasson J. T. (1968) Gallium, germanium, indium and iridium variations in a suite of L-group chondrites. *Geochim. Cosmochim. Acta, 32,* 1087–1110.

Taylor G. J., Keil K., Berkley J. L., and Lance D. E. (1979) The Shaw meteorite: History of a chondrite consisting of impact-melt and metamorphic lithologies. *Geochim. Cosmochim. Acta, 43,* 323–337.

Taylor G. J., Okada A., Scott E. R. D., Rubin A. E., Huss G. R., and Keil K. (1981) The occurrence and implications of carbide-magnetite assemblages in unequilibrated ordinary chondrites (abstract). In *Lunar and Planetary Science XII,* pp. 1076–1078. Lunar and Planetary Institute, Houston.

Taylor G. J., Maggiore P., Scott E. R. D., Rubin A. E., and Keil K. (1987) Original structures, and fragmentation and reassembly histories of asteroids: Evidence from meteorites. *Icarus, 69,* 1–13.

Tonui E., Zolensky M., Lipschutz M., and Okudaira K. (2001) Petrographic and chemical evidence of thermal metamorphism in new carbonaceous chondrites (abstract). *Meteoritics & Planet. Sci., 36,* A207.

Trieloff M., Jessberger E. K., Herrwerth I, Hopp J., Fiéni C., Ghélis M, Bourot-Denise M., and Pellas P. (2003) Structure and thermal history of the H-chondrite parent asteroid revealed by thermochronometry. *Nature, 422,* 502–506.

Van Schmus W. R. and Koffman D. M. (1967) Equilibration temperatures of iron and magnesium in chondritic meteorites. *Science, 155,* 1009–1011.

Van Schmus W. R. and Ribbe P. H. (1969) Composition of phosphate minerals in ordinary chondrites. *Geochim. Cosmochim. Acta, 33,* 637–640.

Van Schmus W. R. and Wood J. A. (1967) A chemical-petrologic classification for the chondritic meteorites. *Geochim. Cosmochim. Acta, 31,* 747–765.

Wasson J. T. (1992) Planetesimal heating by FU-Orionis-Type events (abstract). *Eos Trans. AGU, 73,* 336.

Weisberg M. K., Prinz M., Clayton R. N., and Mayeda T. K. (1997) CV3 chondrites: Three subgroups, not two (abstract). *Meteoritics & Planet. Sci., 32,* A138–A139.

Weisberg M. K., Prinz M., Clayton R. N., Mayeda T. K., Sugiura N., Zashu S., and Ebihara M. (2001) A new metal-rich chondrite grouplet. *Meteoritics & Planet. Sci., 36,* 401–418.

Weisberg M. K., McCoy T. J., and Krot A. N. (2006) Systematics and evaluation of meteorite classification. In *Meteorites and the Early Solar System II* (D. S. Lauretta and H. Y. McSween Jr., eds.), this volume. Univ. of Arizona, Tucson.

Willis J. and Goldstein J. I. (1981) A revision of metallographic cooling rate curves for chondrites. *Proc. Lunar Planet. Sci. 12B,* pp. 1135–1143.

Wlotzka F. (1985) Olivine-spinel and olivine-ilmenite thermometry in chondrites of different petrologic type (abstract). In *Lunar and Planetary Science XVI,* pp. 918–919. Lunar and Planetary Institute, Houston.

Wlotzka F. (1987) Equilibration temperatures and cooling rates of chondrites: A new approach (abstract). *Meteoritics, 22,* 529–531.

Wood J. A. (1962) Metamorphism in chondrites. *Geochim. Cosmochim. Acta, 26,* 739–749.

Wood J. A. (1967) Chondrites: Their metallic minerals, thermal histories, and parent planets. *Icarus, 6,* 1–49.

Wood J. A. and Pellas P. (1991) What heated the meteorite planets? In *The Sun in Time* (C. P. Sonett et al., eds.), pp. 740–760. Univ. of Arizona, Tucson.

Zähringer J. (1968) Rare gases in stony meteorites. *Geochim. Cosmochim. Acta, 32,* 209–237.

Zanda B., Bourot-Denise M., Perron C., and Hewins R. H. (1994) Origin and metamorphic redistribution of silicon, chromium and phosphorus in the metal of chondrites. *Science, 265,* 1846–1849.

Zhang Y., Benoit P. H., and Sears D. W. G. (1995) The classification and complex thermal history of the enstatite chondrites. *J. Geophys. Res., 100,* 9417–9438.

Zhang Y., Huang S., Schneider D., Benoit P. H., DeHart J. M., Lofgren G. E., and Sears D. W. G. (1996) Pyroxene structures, cathodoluminescence and the thermal history of the enstatite chondrites. *Meteoritics & Planet. Sci., 31,* 87–96.

Zolensky M., Abell P., and Tonui E. (2005) Metamorphosed CM and CI carbonaceous chondrites could be from the breakup of the same Earth-crossing asteroid (abstract). In *Lunar and Planetary Science XXXVI,* Abstract #2084. Lunar and Planetary Institute, Houston (CD-ROM).